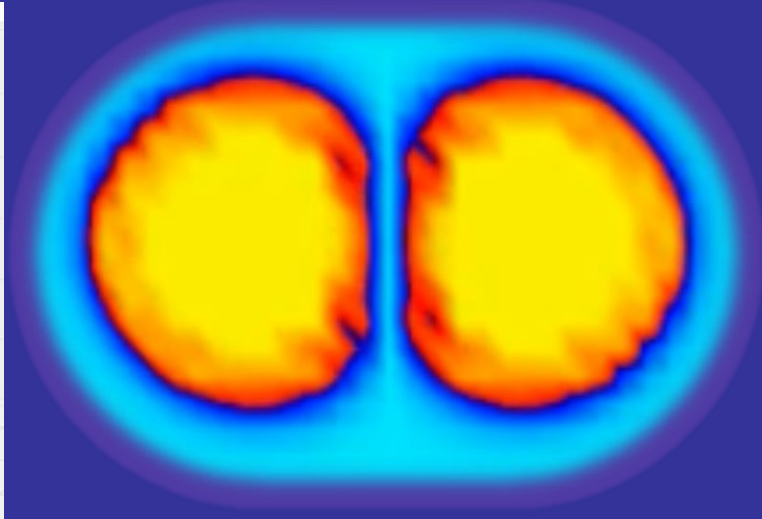
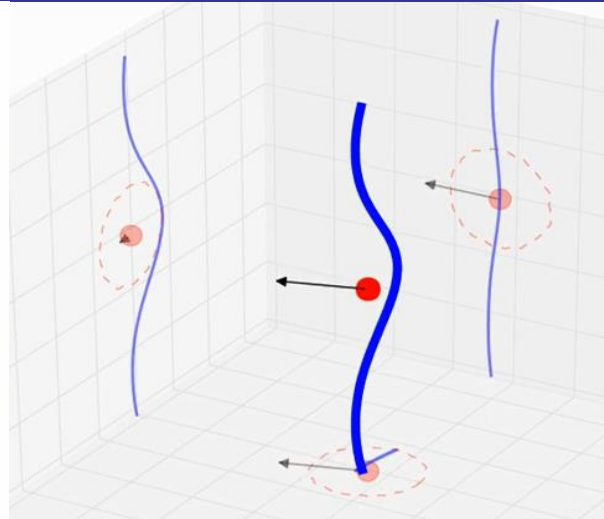
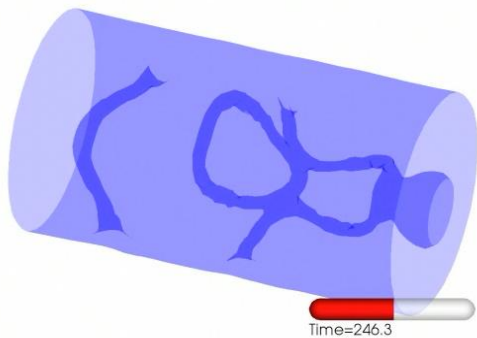


Towards exascale simulations of quantum superfluids far from equilibrium



Piotr Magierski (Warsaw University of Technology)

Collaborators:

Warsaw Univ. of Technology

Janina Grineviciute

Kazuyuki Sekizawa

Gabriel Wlazłowski

Bugra Tuzemen (Ph.D. student)

Konrad Kobuszewski (student)

Aurel Bulgac (Univ. of Washington)

Michael M. Forbes (Washington State U.)

Kenneth J. Roche (PNNL)

Ionel Stetcu (LANL)

Shi Jin (Univ. of Washington, Ph.D. student)

100 years of superconductivity and superfluidity in Fermi systems

Discovery: H. Kamerlingh Onnes in 1911 cooled a metallic sample of mercury at $T < 4.2\text{K}$

20 orders of magnitude over a century of (low temperature) physics

- ✓ Dilute atomic Fermi gases $T_c \approx 10^{-12} - 10^{-9} \text{ eV}$
- ✓ Liquid ^3He $T_c \approx 10^{-7} \text{ eV}$
- ✓ Metals, composite materials $T_c \approx 10^{-3} - 10^{-2} \text{ eV}$
- ✓ Nuclei, neutron stars $T_c \approx 10^5 - 10^6 \text{ eV}$
- QCD color superconductivity $T_c \approx 10^7 - 10^8 \text{ eV}$

units (1 eV \approx 10⁴ K)

Robert B. Laughlin, Nobel Lecture, December 8, 1998:

One of my favorite times in the academic year occurs [...] when I give my class of extremely bright graduate students [...] a take home exam in which they are asked TO DEDUCE SUPERFLUIDITY FROM FIRST PRINCIPLES.

There is no doubt a special place in hell being reserved for me at this very moment for this mean trick, for the task is IMPOSSIBLE. Superfluidity [...] is an **EMERGENT** phenomenon – a low energy collective effect of huge number of particles that CANNOT be deduced from the microscopic equations of motion in a RIGOROUS WAY and that DISAPPEARS completely when the system is taken apart.

[...]students who stay in physics long enough [...] eventually come to understand that the REDUCTIONIST IDEA IS WRONG a great deal of the time and perhaps ALWAYS.

GOAL:

Description of superfluid dynamics of fermionic systems far from equilibrium based on microscopic theoretical framework.

Microscopic framework = explicit treatment of fermionic degrees of freedom.

Why TDDFT?

We need to describe the time evolution of (externally perturbed) spatially inhomogeneous, superfluid Fermi system.

Within current computational capabilities TDDFT allows to describe real time dynamics of strongly interacting, superfluid systems of hundred of thousands fermions.

Other theoretical approaches to superfluid dynamics

Hydrodynamics based on the two-fluid model of Tisza and Landau + extensions.

Based on the assumption that local equilibrium is achieved relatively fast (compared to the observation time).

The microscopic time scale \ll time scale for relaxation of „charges“ (mass density, momentum density, energy density).

No quantization condition for vortices.

Can be treated only as a long-wavelength effective theory.

Gross-Pitaevskii type of equation: based on the concept of a single „wave function“ describing Cooper pair condensate.

Problems: - degrees of freedom leading to deformations of a Fermi sphere are neglected,

- no single-quasiparticle excitations i.e. no mechanism for a dynamically induced transition between a superfluid and a normal state,

- dynamics of vortices (motion and reconnection sequences) is not correct.

Time dependent Ginzburg-Landau approach:

Range of validity is restricted to temperatures very close to T_c .

Microscopic derivations exist only in the limit of gapless superconductivity.

Vortex filament model: Effective theory for topological excitations (quantum vortices) dynamics. Vortices are treated as classical string-like objects of zero thickness.

Microscopic input for various parameters is needed: vortex tension, mass density and interactions. Useful for simulations of quantum turbulence in Bose systems although reconnections have to be put by hand into the description.

Quantum Monte Carlo (QMC)

QMC as an ab-initio method can be used in principle to extract various dynamic properties: eq. viscosity, dynamic spin susceptibility, etc.

Problems: - requires application of linear response theory (Kubo formula)
- requires analytic continuation to convert temperature correlation functions into time correlations. It is numerically an ill-defined problem.

Time dependent Density Functional Theory

Based on Runge Gross mapping

$$i\hbar \frac{\partial}{\partial t} |\psi(t)\rangle = \hat{H} |\psi(t)\rangle, \quad |\psi_0\rangle = |\psi(t_0)\rangle$$

$$\frac{\partial \rho}{\partial t} + \nabla \cdot \vec{j} = 0$$

$$\left. \begin{array}{l} \rho(\vec{r}, t) \\ |\psi(t_0)\rangle \end{array} \right\} \leftrightarrow e^{i\alpha(t)} |\psi(t)\rangle$$

Up to an arbitrary function $\alpha(t)$

and consequently the functional exists:

$$F[\psi_0, \rho] = \int_{t_0}^{t_1} \langle \psi[\rho] | \left(i\hbar \frac{\partial}{\partial t} - \hat{H} \right) | \psi[\rho] \rangle dt$$

E. Runge, E.K.U Gross, PRL 52, 997 (1984)
B.-X. Xu, A.K. Rajagopal, PRA 31, 2682 (1985)
G. Vignale, PRA77, 062511 (2008)

Kohn-Sham approach


Suppose we are given the density of an interacting system.
There exists a unique noninteracting system with the same density.

Interacting system

$$i\hbar \frac{\partial}{\partial t} |\psi(t)\rangle = (\hat{T} + \hat{V}(t) + \hat{W}) |\psi(t)\rangle$$

Noninteracting system

$$i\hbar \frac{\partial}{\partial t} |\varphi(t)\rangle = (\hat{T} + \hat{V}_{KS}(t)) |\varphi(t)\rangle$$


$$\rho(\vec{r}, t) = \langle \psi(t) | \hat{\rho}(\vec{r}) | \psi(t) \rangle = \langle \varphi(t) | \hat{\rho}(\vec{r}) | \varphi(t) \rangle$$

Hence the DFT approach is essentially exact.

However as always there is a price to pay:

- Kohn-Sham potential in principle depends on the past (memory).
Very little is known about the memory term and usually it is disregarded (adiabatic TDDFT).
- Only one body observables can be reliably evaluated within standard DFT.

Superfluid extension of (TD)DFT

Triggered initially by the discovery of high-Tc superconductors:

DFT for superconductors:

L. N. Oliveira, E. K. U. Gross, and W. Kohn, Phys. Rev. Lett. 60 2430 (1988).

TDDFT for superconductors:

O.-J. Wacker, R. Kummel, E.K.U. Gross, Phys. Rev. Lett. 73, 2915 (1994).

Extensions required to introduce an anomalous density:

$$\Delta(\mathbf{r}\sigma, \mathbf{r}'\sigma') = -\frac{\delta E(\rho, \chi)}{\delta \chi^*(\mathbf{r}\sigma, \mathbf{r}'\sigma')}.$$

Problem:

Such formulation results in Kohn-Sham equations in a form of integro-differential equations of enormous computational complexity.

Superfluid Local Density Approximation - Extension of Kohn-Sham approach to superfluid Fermi systems

$$E_{gs} = \int d^3r \varepsilon(n(\vec{r}), \tau(\vec{r}), \nu(\vec{r}))$$

$$n(\vec{r}) = 2 \sum_k |\mathbf{v}_k(\vec{r})|^2, \quad \tau(\vec{r}) = 2 \sum_k |\vec{\nabla} \mathbf{v}_k(\vec{r})|^2$$

$$\nu(\vec{r}) = \sum_k \mathbf{u}_k(\vec{r}) \mathbf{v}_k^*(\vec{r}) \quad \leftarrow \text{pairing (anomalous) density}$$

$$\begin{pmatrix} T + U(\vec{r}) - \mu & \Delta(\vec{r}) \\ \Delta^*(\vec{r}) & -(T + U(\vec{r}) - \mu) \end{pmatrix} \begin{pmatrix} \mathbf{u}_k(\vec{r}) \\ \mathbf{v}_k(\vec{r}) \end{pmatrix} = E_k \begin{pmatrix} \mathbf{u}_k(\vec{r}) \\ \mathbf{v}_k(\vec{r}) \end{pmatrix}$$

Mean-field and pairing field are both local fields!

(for sake of simplicity spin degrees of freedom are not shown)

There is a problem!
The pairing field diverges.

One has to introduce position and momentum dependent running coupling constant.

$$\begin{cases} [h(\vec{r}) - \mu] \mathbf{u}_i(\vec{r}) + \Delta(\vec{r}) \mathbf{v}_i(\vec{r}) = E_i \mathbf{u}_i(\vec{r}) \\ \Delta^*(\vec{r}) \mathbf{u}_i(\vec{r}) - [h(\vec{r}) - \mu] \mathbf{v}_i(\vec{r}) = E_i \mathbf{v}_i(\vec{r}) \end{cases} \quad \begin{cases} h(\vec{r}) = -\vec{\nabla} \frac{\hbar^2}{2m(\vec{r})} \vec{\nabla} + U(\vec{r}) \\ \Delta(\vec{r}) = -g_{\text{eff}}(\vec{r}) \nu_c(\vec{r}) \end{cases}$$

$$\frac{1}{g_{\text{eff}}(\vec{r})} = \frac{1}{g[n(\vec{r})]} - \frac{m(\vec{r}) k_c(\vec{r})}{2\pi^2 \hbar^2} \left\{ 1 - \frac{k_F(\vec{r})}{2k_c(\vec{r})} \ln \frac{k_c(\vec{r}) + k_F(\vec{r})}{k_c(\vec{r}) - k_F(\vec{r})} \right\}$$

$$\rho_c(\vec{r}) = 2 \sum_{E_i \geq 0}^{E_c} |\mathbf{v}_i(\vec{r})|^2, \quad \nu_c(\vec{r}) = \sum_{E_i \geq 0}^{E_c} \mathbf{v}_i^*(\vec{r}) \mathbf{u}_i(\vec{r})$$

$$E_c + \mu = \frac{\hbar^2 k_c^2(\vec{r})}{2m(\vec{r})} + U(\vec{r}), \quad \mu = \frac{\hbar^2 k_F^2(\vec{r})}{2m(\vec{r})} + U(\vec{r})$$

SLDA for unitary Fermi gas

SLDA – Superfluid Local Density Approximation

Fermions at unitarity in a harmonic trap
Total energies $E(N)$

SLDA energy density functional at unitarity

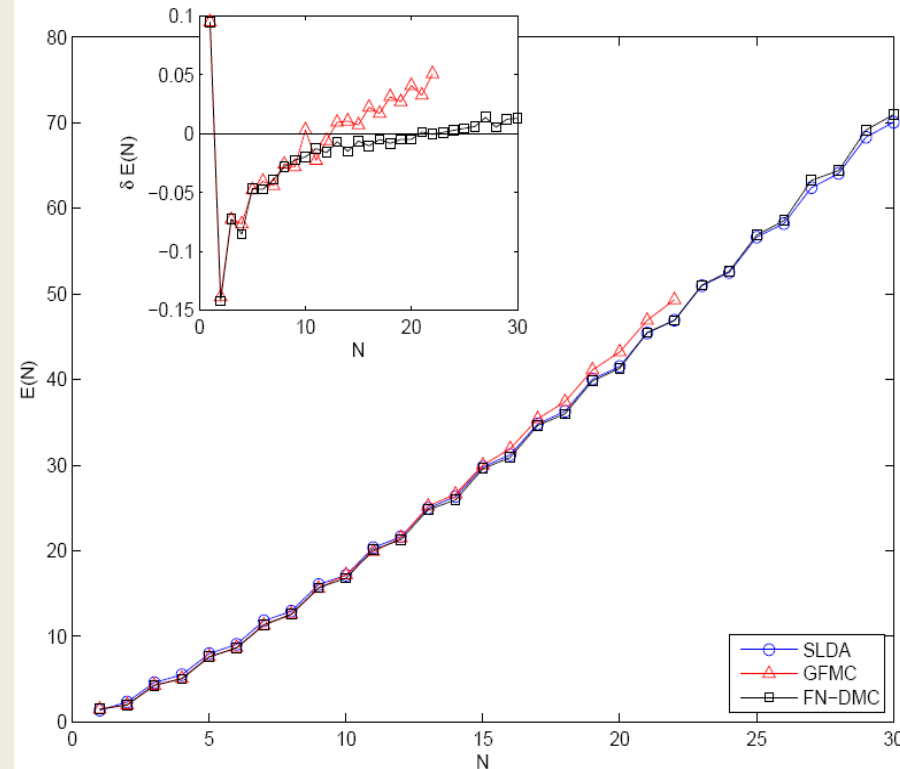
$$\varepsilon(\vec{r}) = \left[\alpha \frac{\tau_c(\vec{r})}{2} - \Delta(\vec{r})\nu_c(\vec{r}) \right] + \beta \frac{3(3\pi^2)^{2/3} n^{5/3}(\vec{r})}{5}$$

$$n(\vec{r}) = 2 \sum_{0 < E_k < E_c} |\psi_k(\vec{r})|^2, \quad \tau_c(\vec{r}) = 2 \sum_{0 < E_k < E_c} |\vec{\nabla} \psi_k(\vec{r})|^2,$$

$$\nu_c(\vec{r}) = \sum_{0 < E_k < E_c} \mathbf{u}_k(\vec{r}) \psi_k^*(\vec{r})$$

$$U(\vec{r}) = \beta \frac{(3\pi^2)^{2/3} n^{2/3}(\vec{r})}{2} - \frac{|\Delta(\vec{r})|^2}{3\gamma n^{2/3}(\vec{r})} + V_{ext}(\vec{r})$$

$$\Delta(\vec{r}) = -g_{eff}(\vec{r})\nu_c(\vec{r})$$



GFMC - Chang and Bertsch, Phys. Rev. A 76, 021603(R) (2007)

FN-DMC - von Stecher, Greene and Blume, PRL 99, 233201 (2007)

PRA 76, 053613 (2007)

Bulgac, PRA 76, 040502(R) (2007)

Normal State				Superfluid State			
(N_a, N_b)	E_{FNDCM}	E_{ASLDA}	(error)	(N_a, N_b)	E_{FNDCM}	E_{ASLDA}	(error)
(3, 1)	6.6 ± 0.01	6.687	1.3%	(1, 1)	2.002 ± 0	2.302	15%
(4, 1)	8.93 ± 0.01	8.962	0.36%	(2, 2)	5.051 ± 0.009	5.405	7%
(5, 1)	12.1 ± 0.1	12.22	0.97%	(3, 3)	8.639 ± 0.03	8.939	3.5%
(5, 2)	13.3 ± 0.1	13.54	1.8%	(4, 4)	12.573 ± 0.03	12.63	0.48%
(6, 1)	15.8 ± 0.1	15.65	0.93%	(5, 5)	16.806 ± 0.04	16.19	3.7%
(7, 2)	19.9 ± 0.1	20.11	1.1%	(6, 6)	21.278 ± 0.05	21.13	0.69%
(7, 3)	20.8 ± 0.1	21.23	2.1%	(7, 7)	25.923 ± 0.05	25.31	2.4%
(7, 4)	21.9 ± 0.1	22.42	2.4%	(8, 8)	30.876 ± 0.06	30.49	1.2%
(8, 1)	22.5 ± 0.1	22.53	0.14%	(9, 9)	35.971 ± 0.07	34.87	3.1%
(9, 1)	25.9 ± 0.1	25.97	0.27%	(10, 10)	41.302 ± 0.08	40.54	1.8%
(9, 2)	26.6 ± 0.1	26.73	0.5%	(11, 11)	46.889 ± 0.09	45	4%
(9, 3)	27.2 ± 0.1	27.55	1.3%	(12, 12)	52.624 ± 0.2	51.23	2.7%
(9, 5)	30 ± 0.1	30.77	2.6%	(13, 13)	58.545 ± 0.18	56.25	3.9%
(10, 1)	29.4 ± 0.1	29.41	0.034%	(14, 14)	64.388 ± 0.31	62.52	2.9%
(10, 2)	29.9 ± 0.1	30.05	0.52%	(15, 15)	70.927 ± 0.3	68.72	3.1%
(10, 6)	35 ± 0.1	35.93	2.7%	(1, 0)	1.5 ± 0.0	1.5	0%
(20, 1)	73.78 ± 0.01	73.83	0.061%	(2, 1)	4.281 ± 0.004	4.417	3.2%
(20, 4)	73.79 ± 0.01	74.01	0.3%	(3, 2)	7.61 ± 0.01	7.602	0.1%
(20, 10)	81.7 ± 0.1	82.57	1.1%	(4, 3)	11.362 ± 0.02	11.31	0.49%
(20, 20)	109.7 ± 0.1	113.8	3.7%	(7, 6)	24.787 ± 0.09	24.04	3%
(35, 4)	154 ± 0.1	154.1	0.078%	(11, 10)	45.474 ± 0.15	43.98	3.3%
(35, 10)	158.2 ± 0.1	158.6	0.27%	(15, 14)	69.126 ± 0.31	62.55	9.5%
(35, 20)	178.6 ± 0.1	180.4	1%				

A. Bulgac, M.M. Forbes, P. Magierski, *in BCS-BEC crossover and the Unitary Fermi gas „Lecture Notes in Physics“ v.836, p. 305, ed. W. Zwerger (2012)*

TDSLDA equations:

Local density approximation

$$i\hbar \frac{\partial}{\partial t} \begin{pmatrix} u_{k\uparrow}(\mathbf{r}, t) \\ u_{k\downarrow}(\mathbf{r}, t) \\ v_{k\uparrow}(\mathbf{r}, t) \\ v_{k\downarrow}(\mathbf{r}, t) \end{pmatrix} = \begin{pmatrix} h_{\uparrow,\uparrow}(\mathbf{r}, t) & h_{\uparrow,\downarrow}(\mathbf{r}, t) & 0 & \Delta(\mathbf{r}, t) \\ h_{\downarrow,\uparrow}(\mathbf{r}, t) & h_{\downarrow,\downarrow}(\mathbf{r}, t) & -\Delta(\mathbf{r}, t) & 0 \\ 0 & -\Delta^*(\mathbf{r}, t) & -h_{\uparrow,\uparrow}^*(\mathbf{r}, t) & -h_{\uparrow,\downarrow}^*(\mathbf{r}, t) \\ \Delta^*(\mathbf{r}, t) & 0 & -h_{\uparrow,\downarrow}^*(\mathbf{r}, t) & -h_{\downarrow,\downarrow}^*(\mathbf{r}, t) \end{pmatrix} \begin{pmatrix} u_{k\uparrow}(\mathbf{r}, t) \\ u_{k\downarrow}(\mathbf{r}, t) \\ v_{k\uparrow}(\mathbf{r}, t) \\ v_{k\downarrow}(\mathbf{r}, t) \end{pmatrix}$$

Density functional contains normal densities, anomalous density (pairing) and currents:

$$E(t) = \int d^3r \left[\varepsilon(n(\vec{r}, t), \tau(\vec{r}, t), \nu(\vec{r}, t), \vec{j}(\vec{r}, t)) + V_{ext}(\vec{r}, t)n(\vec{r}, t) + \dots \right]$$

- The system is placed on a large 3D spatial lattice.
- No symmetry restrictions
- Number of PDEs is of the order of the number of spatial lattice points

The main advantage of TDSLDA over TDHF (+TDBCS) is related to the fact that in TDSLDA the pairing correlations are described as a true complex field which has its own modes of excitations, which include spatial variations of both amplitude and phase. Therefore in TDSLDA description the evolution of nucleon Cooper pairs is treated consistently with other one-body degrees of freedom.

Current capabilities of the code:

- volumes of the order of ($L = 100^3$) capable of simulating time evolution of about 150000 neutrons at saturation density (natural application: neutron stars)
- capable of simulating up to times of the order of 10^{-19} s (a few million time steps)
- CPU vs GPU on Titan (16 CPUs per 1 GPU)

Table 1: Comparison of profit gained by using GPUs instead of CPUs for two example lattices. The timing was obtained on Titan supercomputer. Note, Titan has 16x more CPUs than GPUs.

$N_x N_y N_z$	Number of HFB equations	CPU implementation		GPU implementation		SPEEDUP
		# of CPUs	time per step	# of GPUs	time per step	
48^3	110,592	110,592	3.9 sec	6,912	0.39 sec	10
64^3	<u>262,144</u>	262,144	20 sec	16,384	0.80 sec	25



Over 1 million time-dependent 3D nonlinear complex coupled PDEs

Cray XK7, ranked at peak ≈ 27 Petaflops (Peta – 10^{15})

*On Titan there are 18,688 GPUs which provide 24.48 Petaflops !!!
and 299,008 CPUs which provide only 2.94 Petaflops.*

A single GPU on Titan performs the same amount of FLOPs as approximately 134 CPUs.

Areas of applications

**Ultracold atomic
(fermionic) gases.**

Unitary regime.

Dynamics of vortices,
solitonic excitations,
quantum turbulence.

$$\frac{\Delta}{\mathcal{E}_F} \leq 0.5$$

Nuclear physics.

Induced nuclear
fission, fusion,
collisions.

$$\frac{\Delta}{\mathcal{E}_F} \leq 0.03$$

**Astrophysical
applications.**

Modelling of neutron star
interior (glitches): vortex
dynamics, dynamics of
inhomogeneous nuclear
matter.

$$\frac{\Delta}{\mathcal{E}_F} \leq 0.1 - 0.2$$

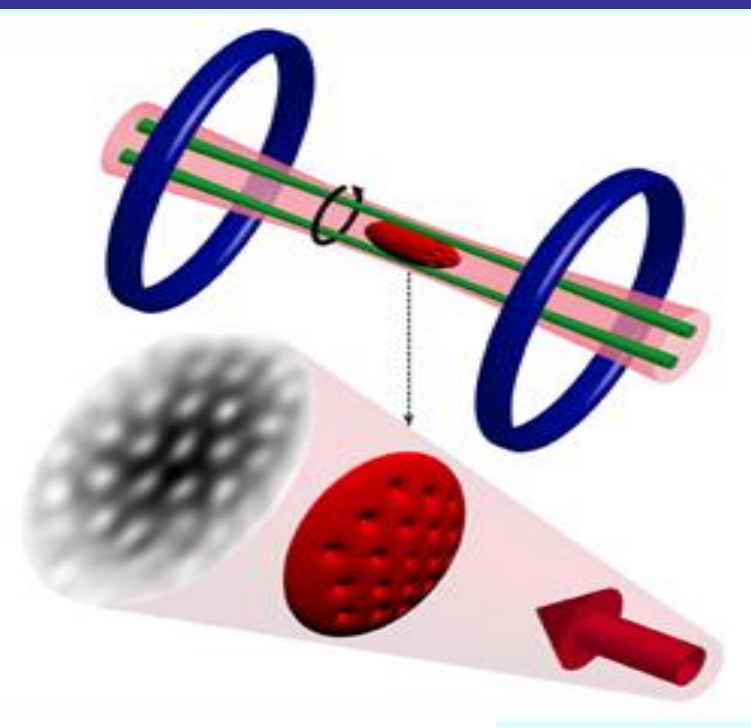
Topological excitations in ultracold Fermi gases

Short (selective) history:

- ✓ In 1999 DeMarco and Jin created a degenerate atomic Fermi gas.
- ✓ In 2005 Zwierlein/Ketterle group observed quantum vortices which survived when passing from BEC to unitarity - evidence for superfluidity!

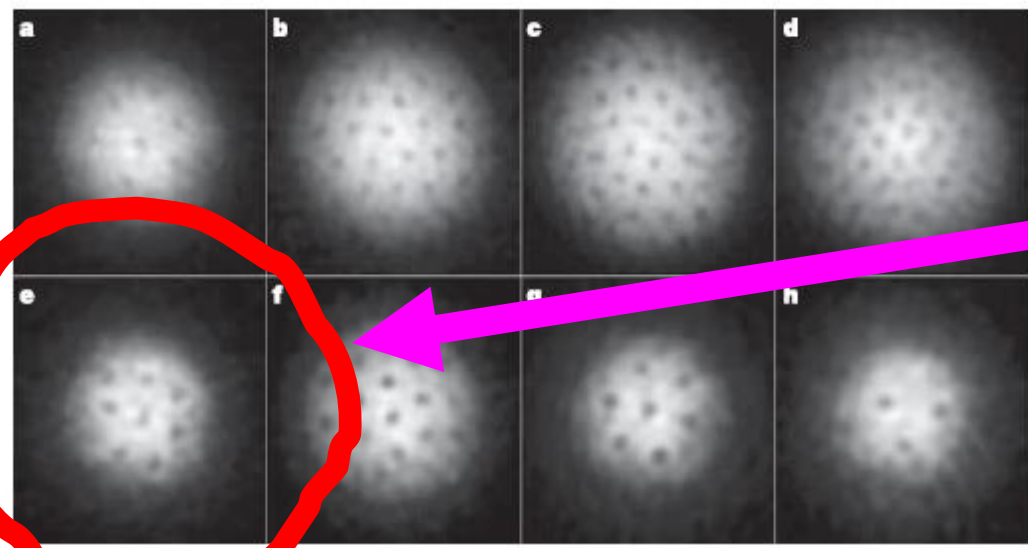
system of fermionic ${}^6\text{Li}$ atoms

Feshbach resonance: $B=834\text{G}$



BEC side:
 $a > 0$

BCS side:
 $a < 0$



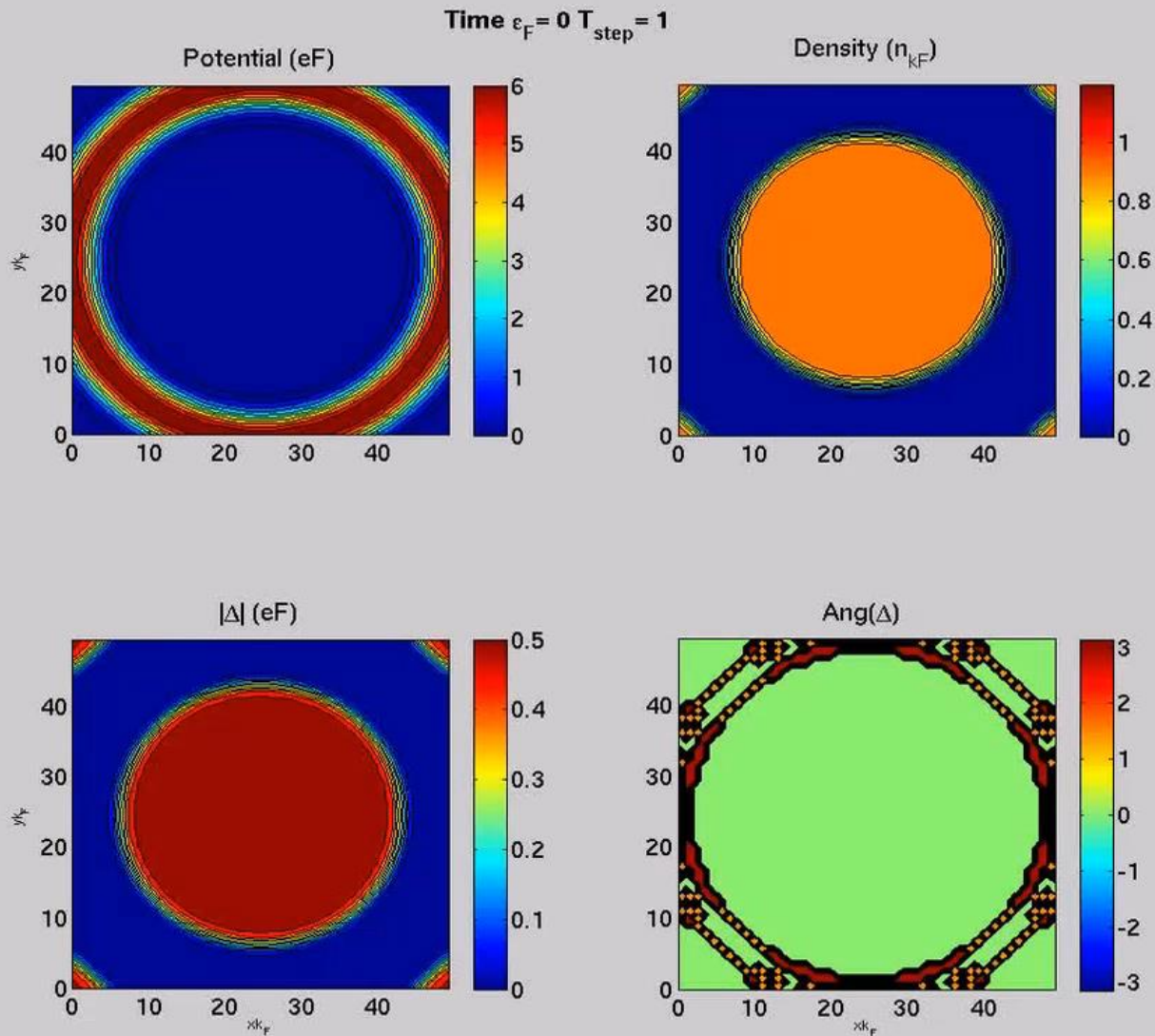
UNITARY REGIME

Figure 2 | Vortices in a strongly interacting Fermionic atoms on the BEC- and the BCS-side of the Feshbach resonance. At the given field, the cloud of lithium atoms was stirred for 300 ms (a) or 500 ms (b–h) followed by an equilibration time of 500 ms. After 2 ms of ballistic expansion, the

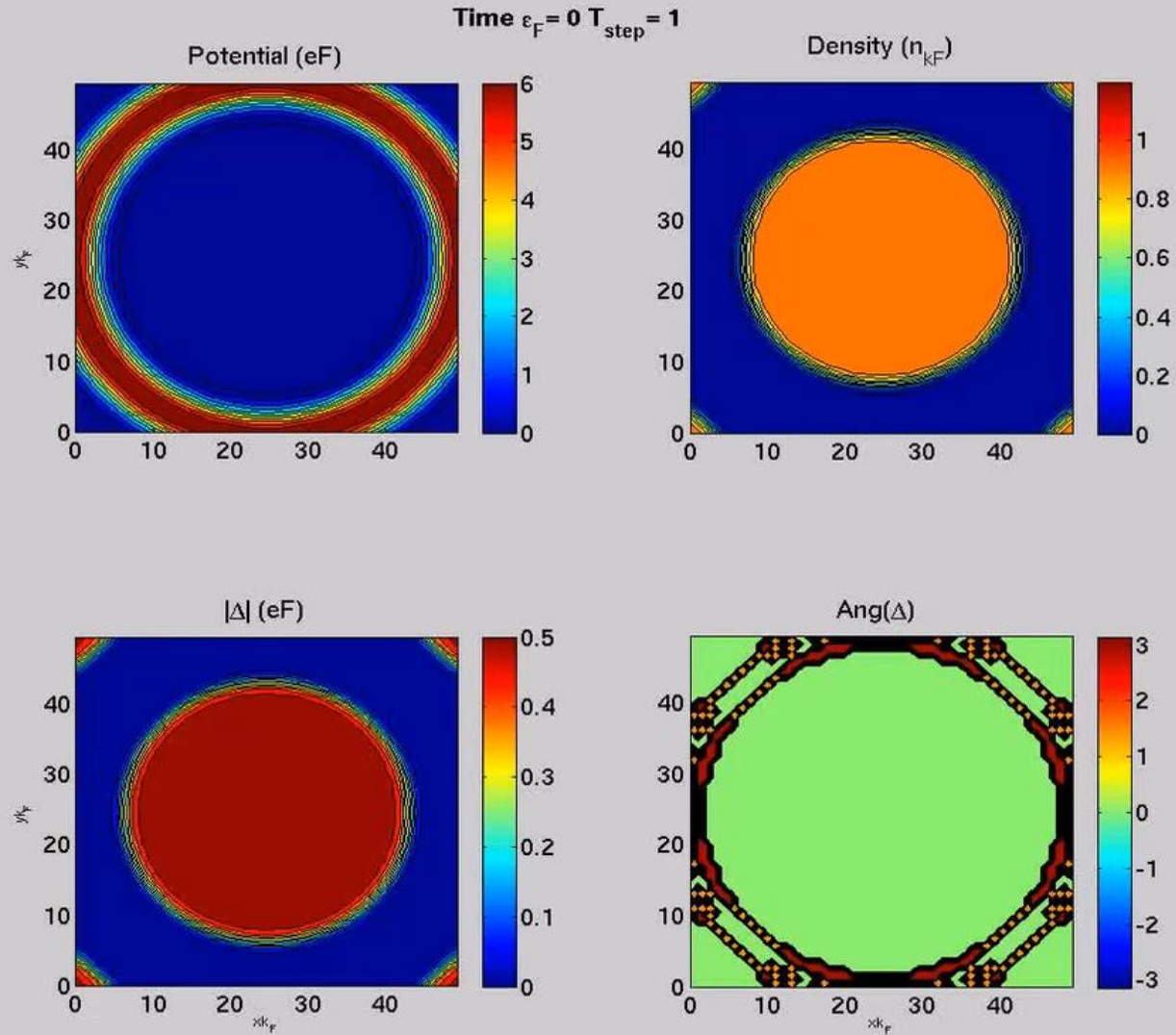
magnetic field was ramped to 735 G for imaging (see Methods). The magnetic fields were 740 G (a), 766 G (b), 792 G (c), 843 G (f), 853 G (g) and 863 G (h). The field of view is $880 \mu\text{m} \times 880 \mu\text{m}$.

M.W. Zwierlein et al., Nature, 435, 1047 (2005)

Stirring the atomic cloud with stirring velocity **lower** than the critical velocity



Stirring the atomic cloud with stirring velocity **exceeding** the critical velocity



Vortex reconnections

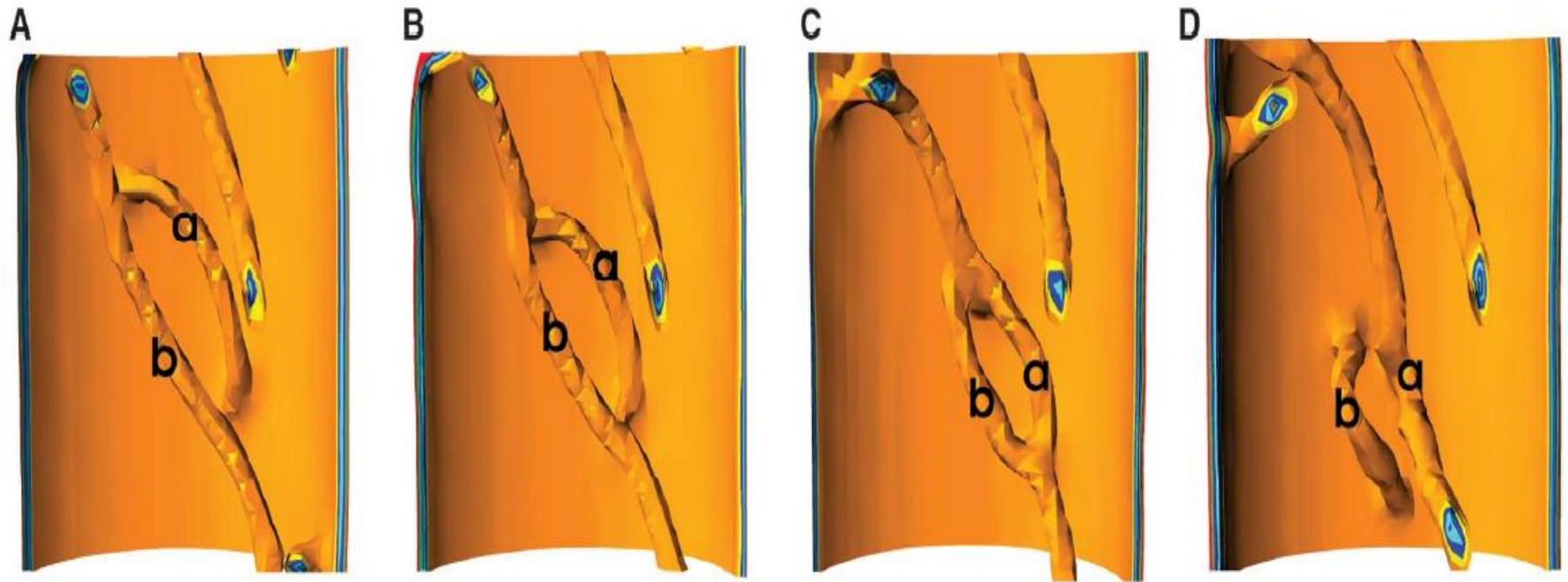
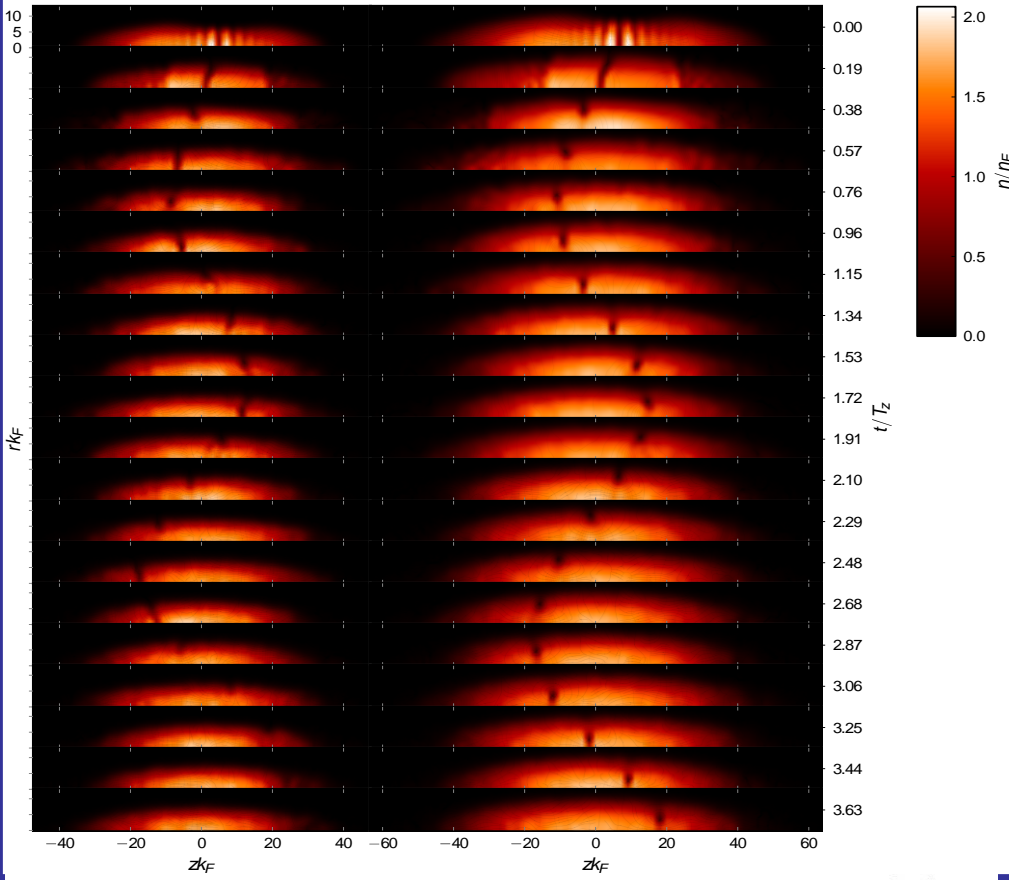
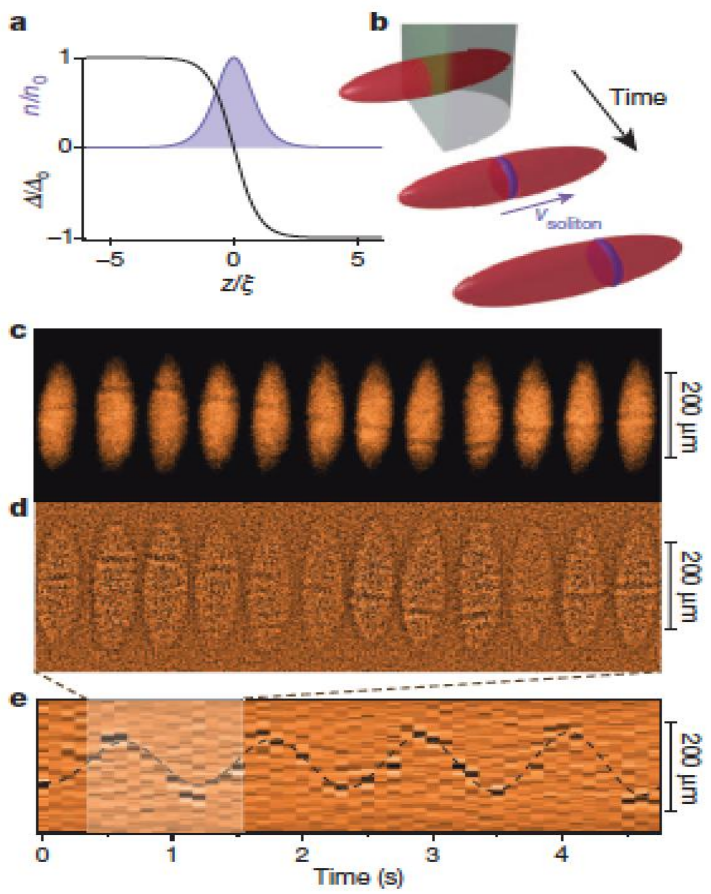


Fig. 3. (A to D) Two vortex lines approach each other, connect at two points, form a ring and exchange between them a portion of the vortex line, and subsequently separate. Segment (a), which initially belonged to the vortex line attached to the wall, is transferred to the long vortex line (b) after reconnection and vice versa.

Vortex reconnections are important for the energy dissipation mechanism in quantum turbulence.

TDSLDA can describe these processes as well as the energy transfer between collective and single particle degrees of freedom (which is a problem for simplified treatments based e.g. on Gross-Pitaevskii equation)

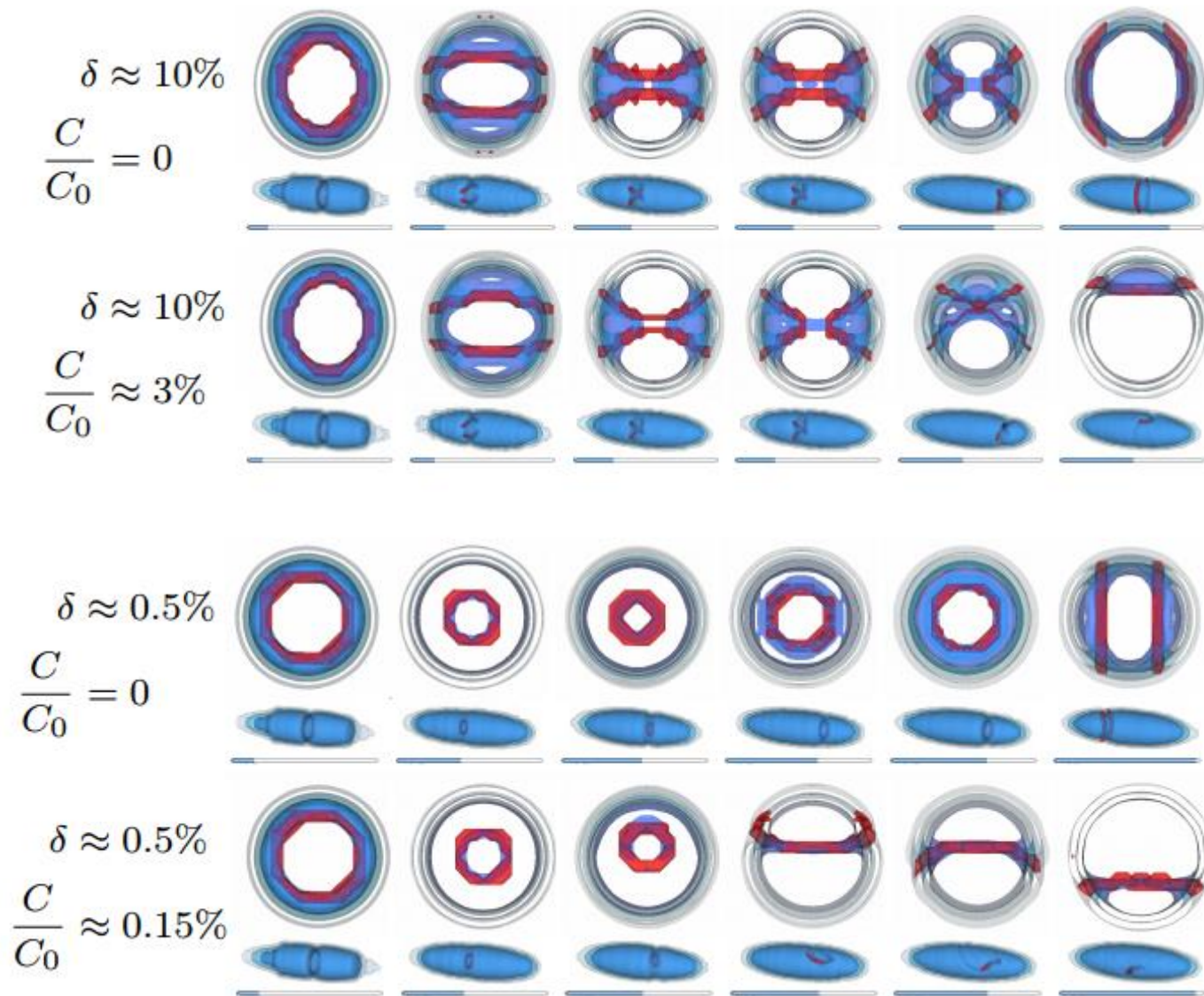
A great example on how TDSLDA help clarify a great puzzle and give a correct interpretation to an experimental result. The "heavy soliton" proved to be a vortex ring.



PRL 112, 025301 (2014) PHYSICAL REVIEW LETTERS week ending 17 JANUARY 2014
Quantized Superfluid Vortex Rings in the Unitary Fermi Gas
 Aurel Bulgac,¹ Michael McNeil Forbes,^{2,1,3} Michelle M. Kelley,⁴ Kenneth J. Roche,^{5,1} and Gabriel Wlazowski^{6,1}

Heavy solitons in a fermionic superfluid
 Tarik Yefsah¹, Ariel T. Sommer¹, Mark J. H. Ku¹, Lawrence W. Cheuk¹, Wenjie Ji¹, Waseem S. Bakr² & Martin W. Zwierlein¹

Nature, 429, 426-430 (2013)



Moreover with TDDFT we can reproduce the sequence of topological excitations observed experimentally (M.H.J. Ku et al. Phys. Rev. Lett. 113, 065301 (2014)).

Road to quantum turbulence

Classical turbulence: energy is transferred from large scales to small scales where it eventually dissipates.

Kolmogorov spectrum: $E(k) = C \varepsilon^{2/3} k^{-5/3}$

E – kinetic energy per unit mass associated with the scale $1/k$

ε - energy rate (per unit mass) transferred to the system at large scales.

k - wave number (from Fourier transformation of the velocity field).

C – dimensionless constant.

Superfluid turbulence (quantum turbulence): disordered set of quantized vortices. The friction between the superfluid and normal part of the fluid serves as a source of energy dissipation.

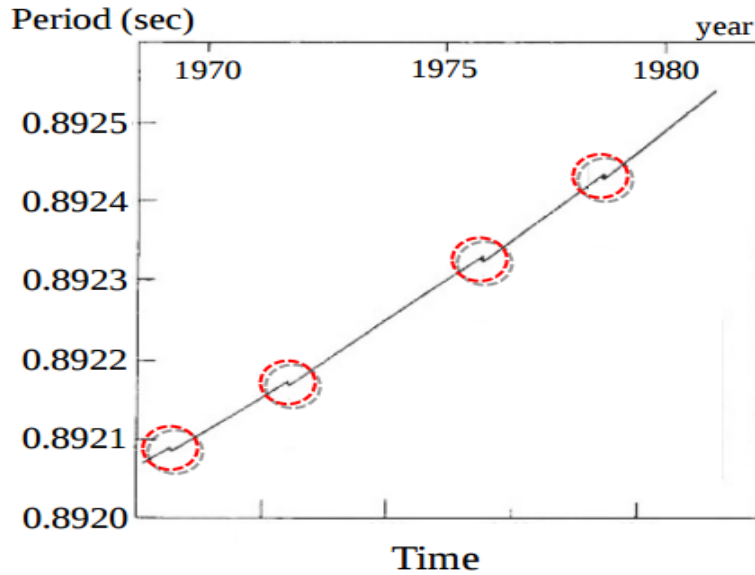
Problem: how the energy is dissipated in the superfluid system at small scales at $T=0$? - „pure“ quantum turbulence

Possibility: vortex reconnections \rightarrow Kelvin waves \rightarrow phonon radiation

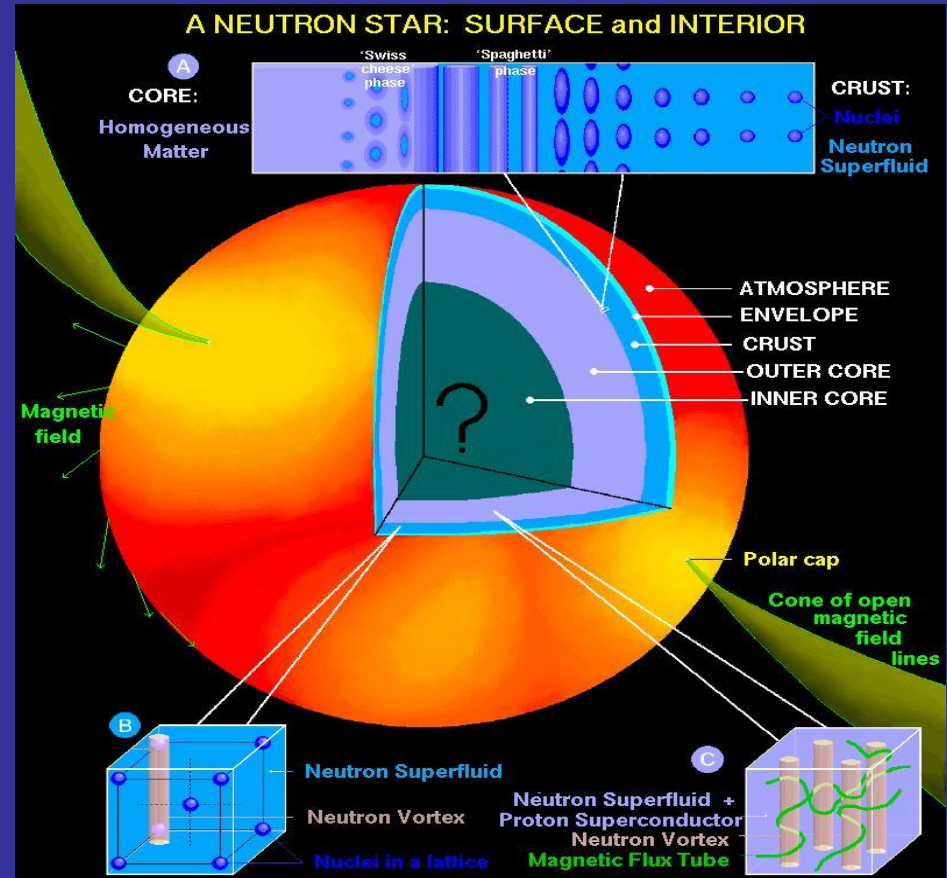
Modelling neutron star interior

Glitch: a sudden increase of the rotational frequency

Glitches in the Vela pulsar



V.B. Bhatia, A Textbook of Astronomy and Astrophysics with Elements of Cosmology, Alpha Science, 2001.



glitch phenomenon=a sudden speed up of rotation.
To date more than 300 glitches have been detected in more than 100 pulsars

Glitch phenomenon is commonly believed to be related to rearrangement of vortices in the interior of neutron stars. It would require however a correlated behavior of huge number of quantum vortices and the mechanism of such collective rearrangement is still a mystery.

To date the impurity-vortex interaction has been extracted from static calculations (Ginzburg-Landau, local density, HFB) with several severe approximations:

- Vortex is always straight
- Nucleus is spherical
- Only very symmetric configurations are considered:
 - nucleus on vortex
 - vortex inbetween two nuclei (interstitial configuration)
 - nucleus at infinity

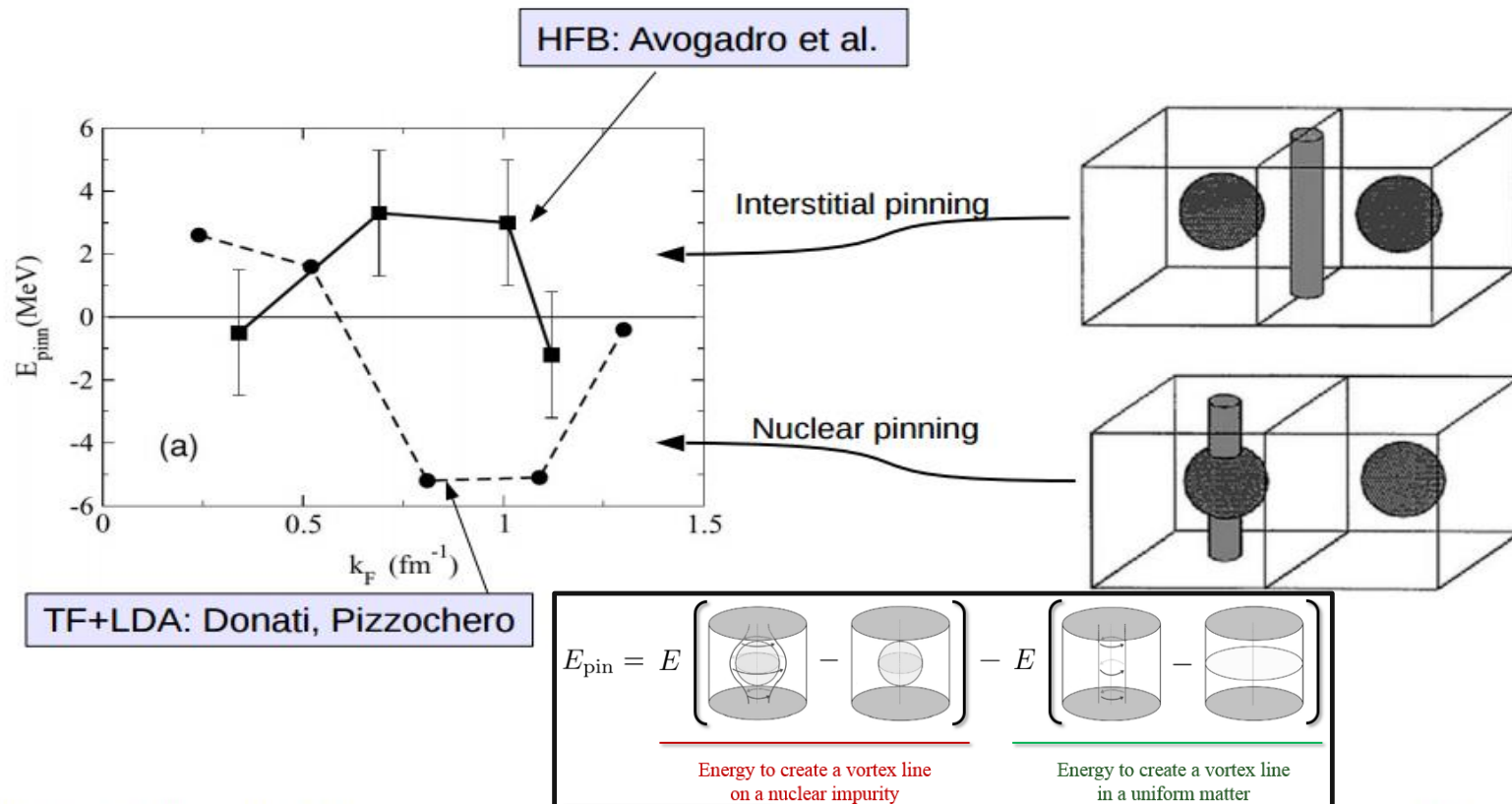


Fig. from: P. Avogadro et al., Phys. Rev. C 75, 012805(R) (2007)

Figs from: P. Donati et al., Nuclear Physics A 742 (2004) 363

Vortex dynamics and vortex-impurity interaction

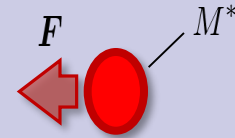
The effective equations of motion for the vortex dynamics (per unit length of the vortex):

$$M_{\text{vor}} \frac{d^2 \vec{r}}{dt^2} = \vec{F}_M + \vec{F}_D + \vec{F}_{\text{vor-impurity}}$$

Superfluid neutrons

Vortex tension

Effective mass



$$\vec{F}_M = \rho_s \vec{\Gamma} \times \left(\frac{d\vec{r}}{dt} - \vec{v}_s \right) - \text{Magnus force; } \vec{\Gamma} - \text{local vorticity;}$$

$\frac{d\vec{r}}{dt}$ - local vortex velocity, ρ_s - superfluid density, \vec{v}_s - superfluid velocity

\vec{F}_D - frictional force (negligible at small T)

$\vec{F}_{\text{vor-impurity}}$ - vortex-impurity force

How to extract the force

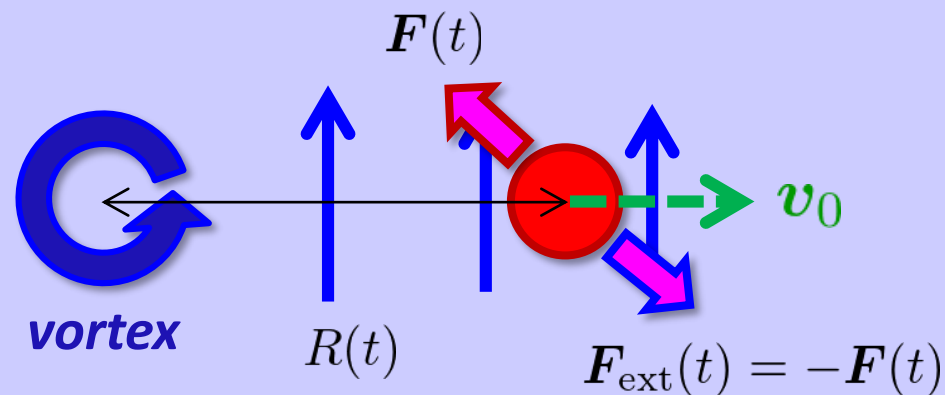
We directly measure the force $F(R)$ in dynamical simulation

- Newton's law

$$F = M \frac{dv}{dt} \quad \rightarrow \quad \frac{dv}{dt} = 0 \quad \text{if} \quad F = 0$$

- We keep a nuclear motion in a constant velocity v_0 ($\ll v_{\text{crit}}$)

Superfluid neutrons



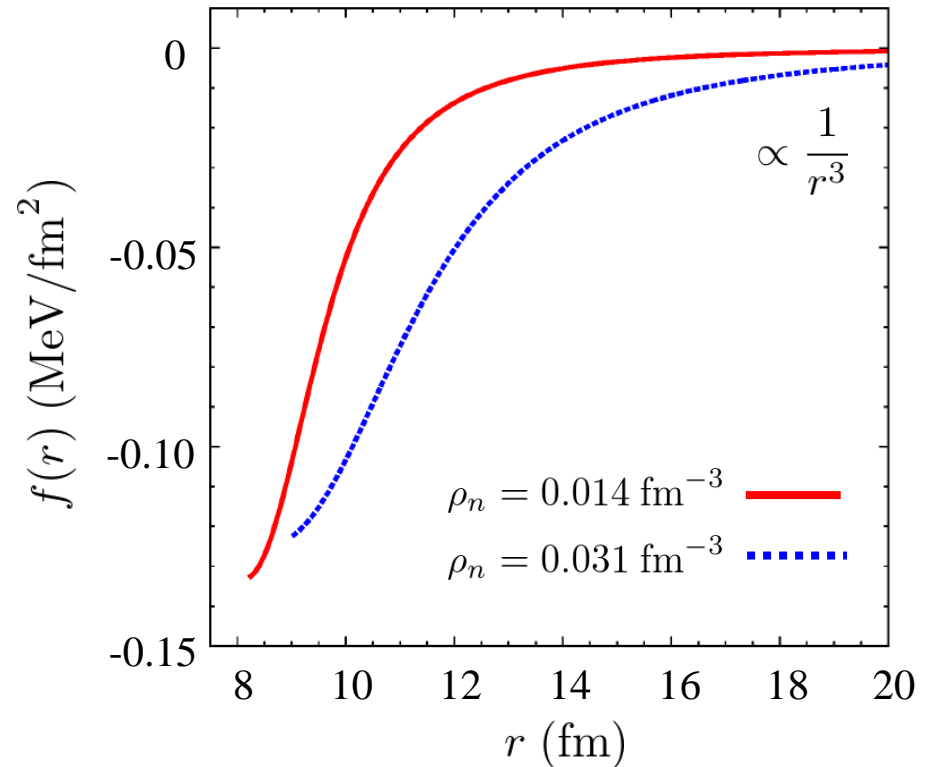
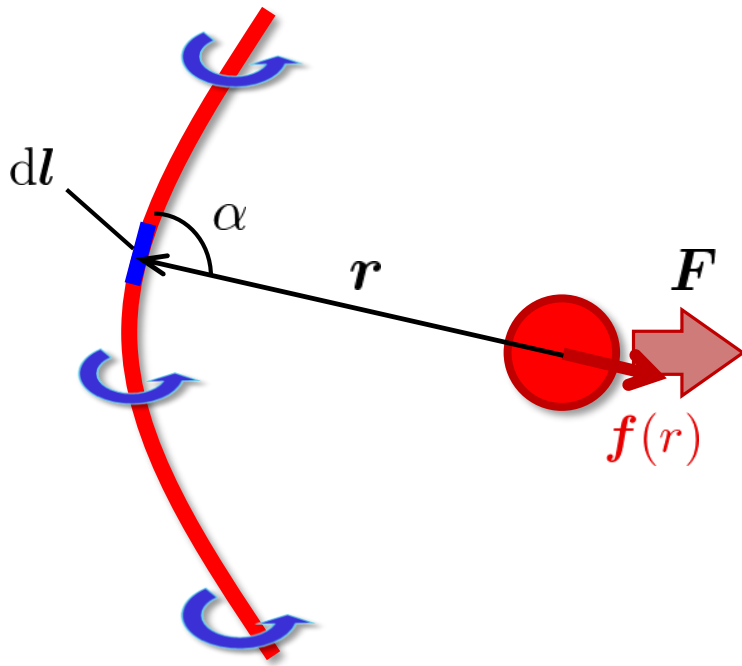
Force per unit length

We can predict the force for any vortex-nucleus configuration

➤ Force per unit length

$$\mathbf{F} = \int_L f(r) \sin \alpha \mathbf{e}_r dl$$

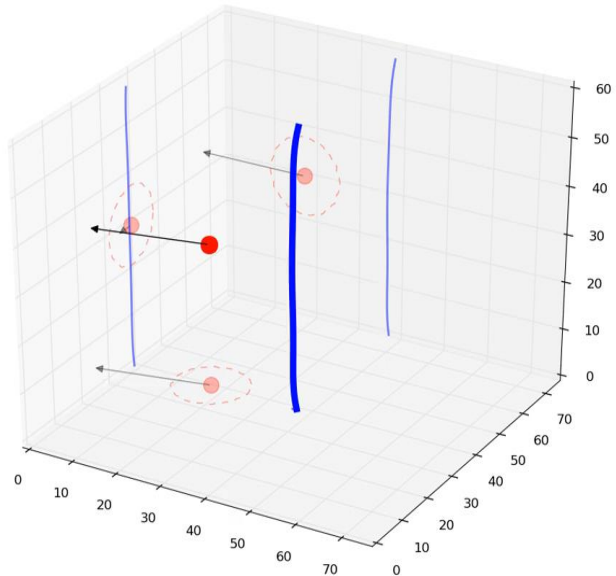
$$f(r) = \frac{\sum_{k=0}^n a_k r^k}{1 + \sum_{k=1}^{n+3} b_k r^k} \quad \text{Padé approximant (n=2 was used)}$$



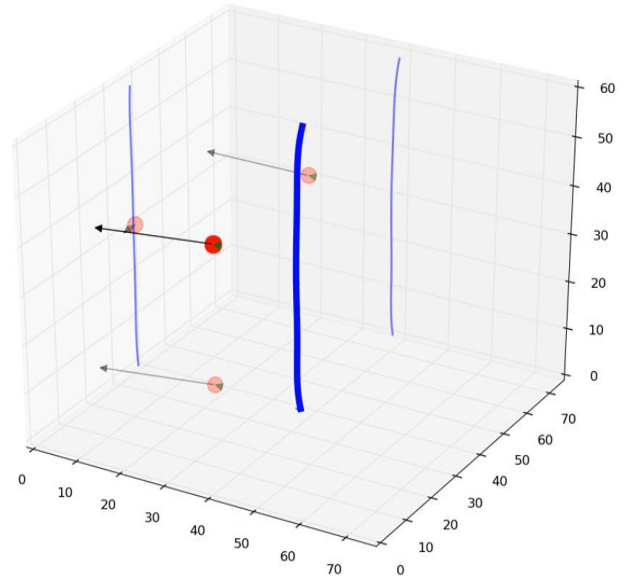
Vortex – impurity interaction

The external potential keeps the nucleus moving along the straight line with a constant velocity below the critical velocity.

time= 0 fm/c
F(19.1)= 2.08 MeV/fm
Q= 28.0fm²



time= 11 fm/c
F_m(19.1)= 2.08 MeV/fm
F_t(19.1)= 0.01 MeV/fm



Effective mass of a nucleus in superfluid neutron environment

Suppose we would like to evaluate an effective mass of a heavy particle immersed in a Fermi bath.

It means we would like to replace the original problem with the simplified equation:

$$i\hbar \frac{\partial}{\partial t} \Psi = \hat{H} \Psi \quad \xrightarrow{?} \quad M \frac{d^2 q}{dt^2} - F_D \left(\frac{dq}{dt}, \dots \right) + \frac{dE}{dq} = 0$$

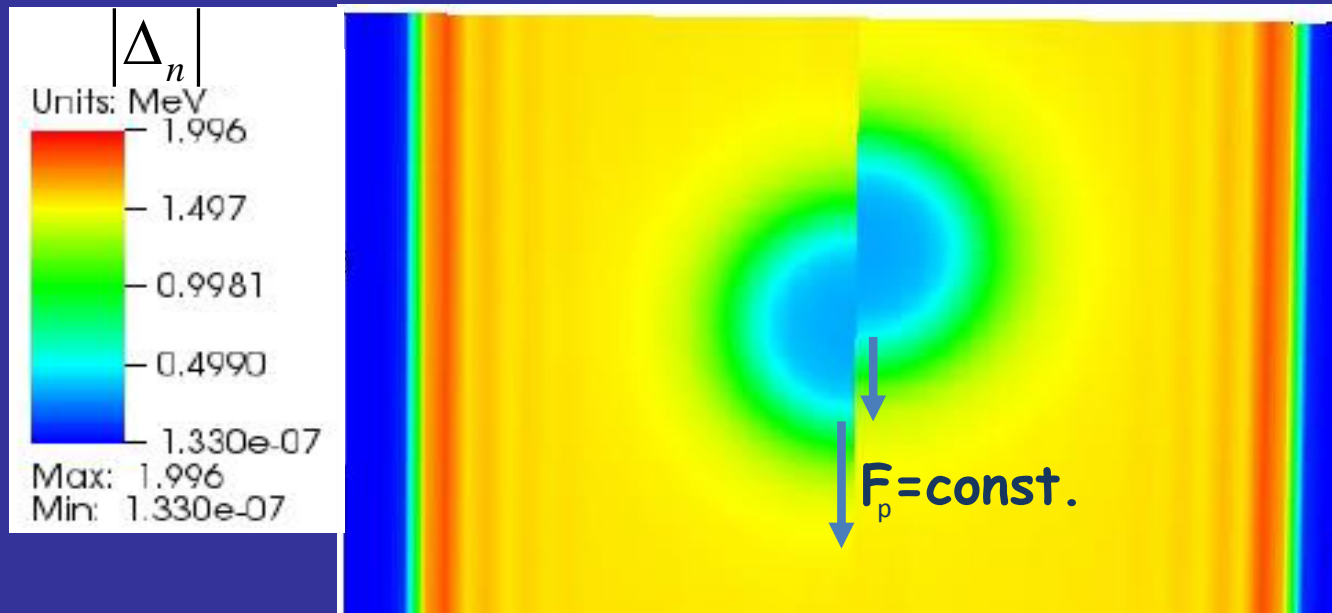
In general it is a complicated task as the first (mass term) and the second term (dissipation) may not be unambiguously separated.

However, for the superfluid system it can be done as for sufficiently slow motion (below the critical velocity) the second term may be neglected due to the presence of the pairing gap.

Another difficulty:

In the context of the neutron star crust it is also not known a priori what is the effective size of the moving impurity, ie. how many neutrons will be dragged.

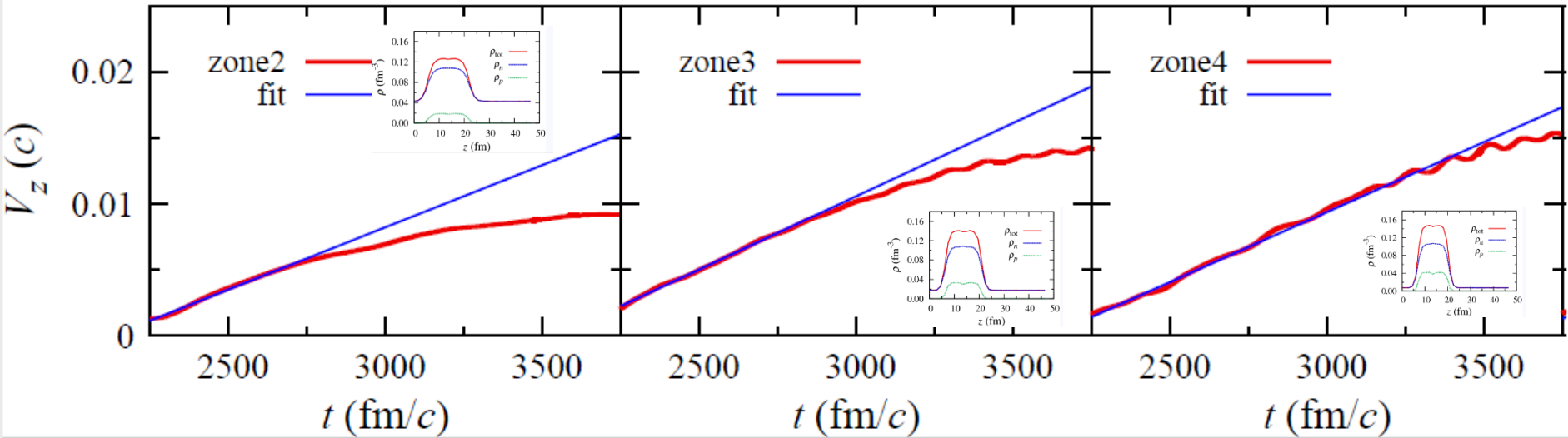
Determination of nuclear effective mass in the superfluid neutron environment from time dependent DFT:



$$M_{eff} = \frac{F_p}{\left(\frac{dV_{CM \text{ protons}}}{dt} \right)}$$

Exerting a constant force on protons we measure the velocity of the proton CM as a function of time and determine the mass.

Velocity of protons for various zones in neutron star crust ($F = 2 \text{ MeV/fm}$)



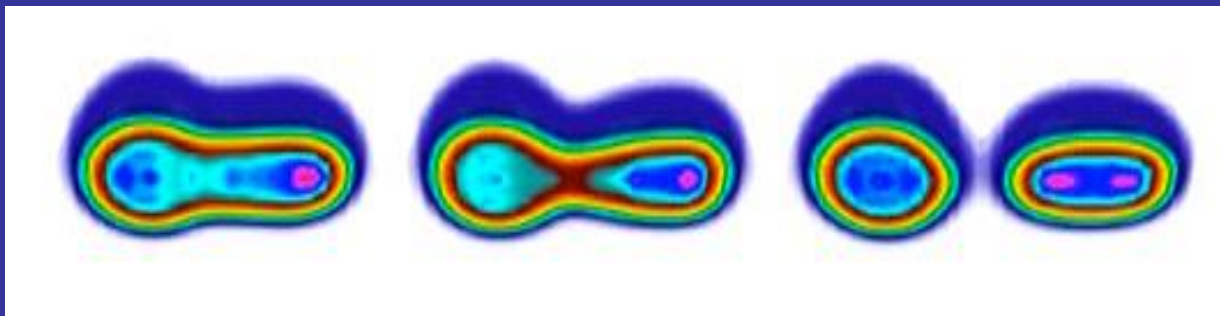
Advantages:

- Size of impurity is selfconsistently determined.
- No need to specify boundary conditions between impurity and superfluid environment.
- No need to divide the system into bound and unbound neutrons.
- No ambiguities concerning relation between superfluid density (which enters hydrodyn. description) and neutron and proton densities.
- Adding other obstacles/impurities is straightforward.
- The critical velocity at which dissipative effects set in can be extracted.
- Various collective degrees of freedom involving impurity itself (eg. deformation) and its coupling to the environment are selfconsistently included.
- This approach offers an easy way to determine important collective modes, which may be excited by moving impurity (for example: we have detected low lying isovector GDR at energies of about 1 MeV).

Zone	Element	Z	N	R_{WS} [fm]	ρ_b [$\text{g} \cdot \text{cm}^{-3}$]	$k_{F,n}$ [fm^{-1}]
11	^{180}Zr	40	140	53.6	$4.67 \cdot 10^{11}$	0.12
10	^{200}Zr	40	160	49.2	$6.69 \cdot 10^{11}$	0.15
9	^{250}Zr	40	210	46.4	$1.00 \cdot 10^{12}$	0.19
8	^{320}Zr	40	280	44.4	$1.47 \cdot 10^{12}$	0.23
7	^{500}Zr	40	460	42.2	$2.66 \cdot 10^{12}$	0.31
6	^{950}Sn	50	900	39.3	$6.24 \cdot 10^{12}$	0.43
5	^{1100}Sn	50	1050	35.7	$9.65 \cdot 10^{12}$	0.51
4	^{1350}Sn	50	1300	33.0	$1.49 \cdot 10^{13}$	0.60
3	^{1800}Sn	50	1750	27.6	$3.41 \cdot 10^{13}$	0.80
2	^{1500}Zr	40	1460	19.6	$7.94 \cdot 10^{13}$	1.08
1	^{982}Ge	32	950	14.4	$1.32 \cdot 10^{14}$	1.33

Pastore,Baroni,Losa, arXiv:1108.3123

Nuclear physics applications: Induced Fission of ^{240}Pu

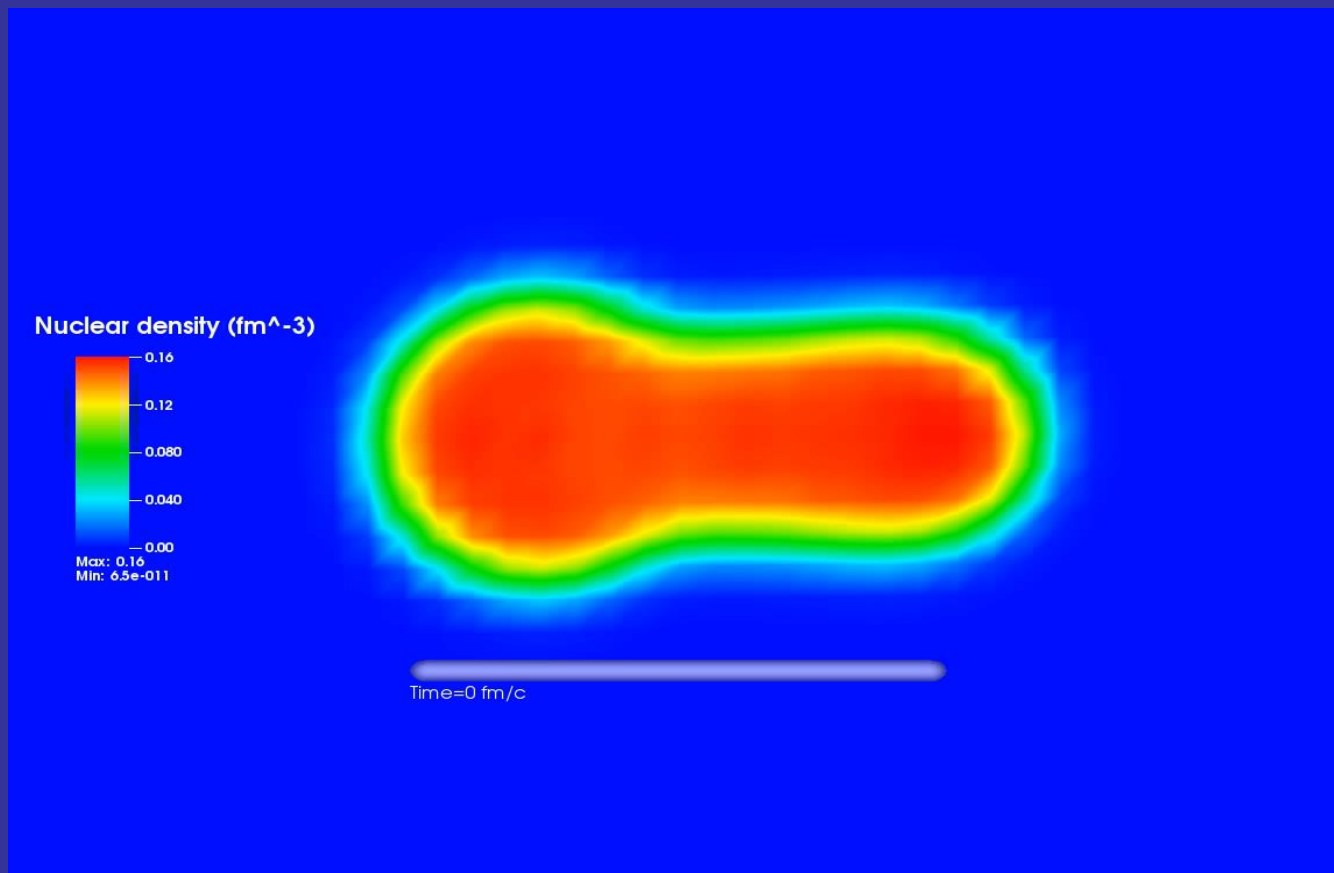


Advantages of TDDFT for large amplitude nuclear motion

- No need to introduce and to guess the number and character of collective variables. The number of excited shape degrees of freedom is large and it increases during the evolution. This makes treatments like GCM, based on a fix number of collective coordinates quite doubtful.
- No need to evaluate the rather ill-defined potential energy surface. *Not clear how to choose the collective coordinates, how to choose the constraints, how to choose their number, and whether to require the nucleus to be cold or not.*
- No need to determine the rather ill-defined inertia tensor. *Several prescriptions are used in literature.*
- There is no need to invoke (or not) adiabaticity, since as a matter of fact the dynamical evolution is not close to equilibrium, at either zero or at a finite temperature. The evolution is truly a non-equilibrium one.
- One-body dissipation, the window and wall dissipation mechanisms are automatically incorporated into the theoretical framework.
- No modeling (except for the energy density functional, which so far is tested in completely unrelated conditions and which has a relative accuracy of $\approx 10^{-3}$).
- All shapes are allowed and the nucleus chooses dynamically the path in the shape space, the forces acting on nucleons are determined by the nucleon distributions and velocities, and the nuclear system naturally and smoothly evolves into separated fission fragments.
- There is no need to introduce such unnatural quantum mechanical concepts as "rupture" and there is no worry about how to define the scission configuration.
- One can extract difficult to gain otherwise information: angular momentum distribution and excitation energies of the fission fragments,

Complexity of fission dynamics

Initial configuration of ^{240}Pu is prepared beyond the barrier at quadrupole deformation $Q=165b$ and excitation energy $E=8.08\text{ MeV}$:

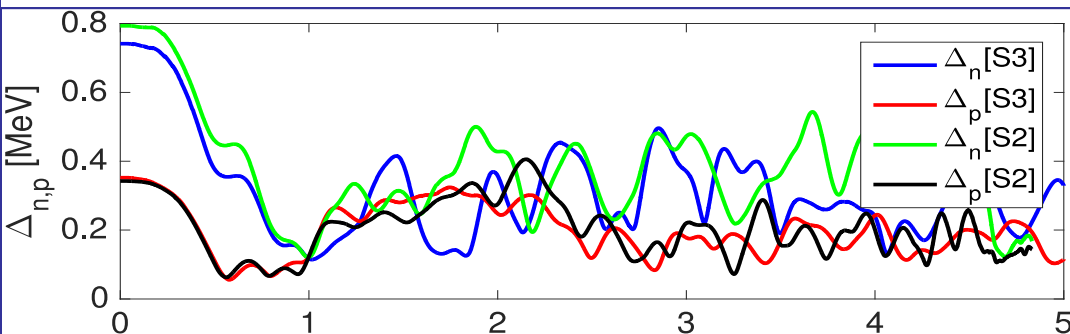


During the process shown, the exchange of about 2 neutrons and 3 protons occur between fragments before the actual fission occurs.

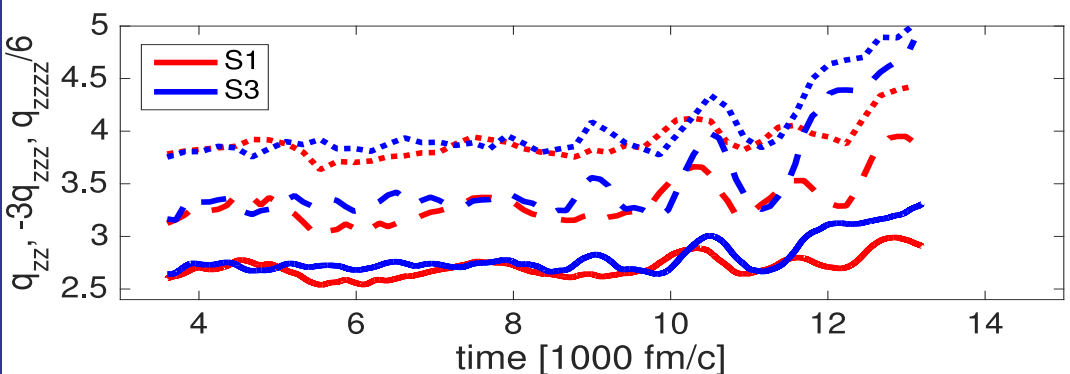
Interestingly the fragment masses seem to be relatively stiff with respect to changes of the initial conditions.

TABLE I. The simulation number, the pairing parameter η , the excitation energy (E^*) of $^{240}\text{Pu}_{146}$ and of the fission fragments [$E_{H,L}^* = E_{H,L}(t_{\text{SS}}) - E_{gs}(N_{H,L}, Z_{H,L})$], the equivalent neutron incident energy (E_n), the scaled initial mass moments $q_{20}(0)$ and $q_{30}(0)$, the ‘‘saddle-to-scission’’ time t_{SS} , TKE evaluated as in Ref. [71], TKE, atomic (A_L^{syst}), neutron (N_L^{syst}), and proton (Z_L^{syst}) extracted from data [72] using Wahl’s charge systematics [73] and the corresponding numbers obtained in simulations, and the number of postscission neutrons for the heavy and light fragments ($\nu_{H,L}$), estimated using a Hauser-Feshbach approach and experimental neutron separation energies [8,74,75]. Units are in MeV, fm², fm³, fm/c as appropriate.

S no.	η	E^*	E_n	q_{zz}	q_{zzz}	t_{SS}	TKE ^{syst}	TKE	A_L^{syst}	A_L	N_L^{syst}	N_L	Z_L^{syst}	Z_L	E_H^*	E_L^*	ν_H	ν_L
S1	0.75	8.05	1.52	1.78	-0.742	14 419	177.27	182	100.55	104.0	61.10	62.8	39.45	41.2	5.26	17.78	0	1.9
S2	0.5	7.91	1.38	1.78	-0.737	4360	177.32	183	100.56	106.3	60.78	64.0	39.78	42.3	9.94	11.57	1	1
S3	0	8.08	1.55	1.78	-0.737	14 010	177.26	180	100.55	105.5	60.69	63.6	39.81	41.9	3.35	29.73	0	2.9
S4	0	6.17	-0.36	2.05	-0.956	12 751	177.92	181		103.9		62.6		41.3	7.85	9.59	1	1

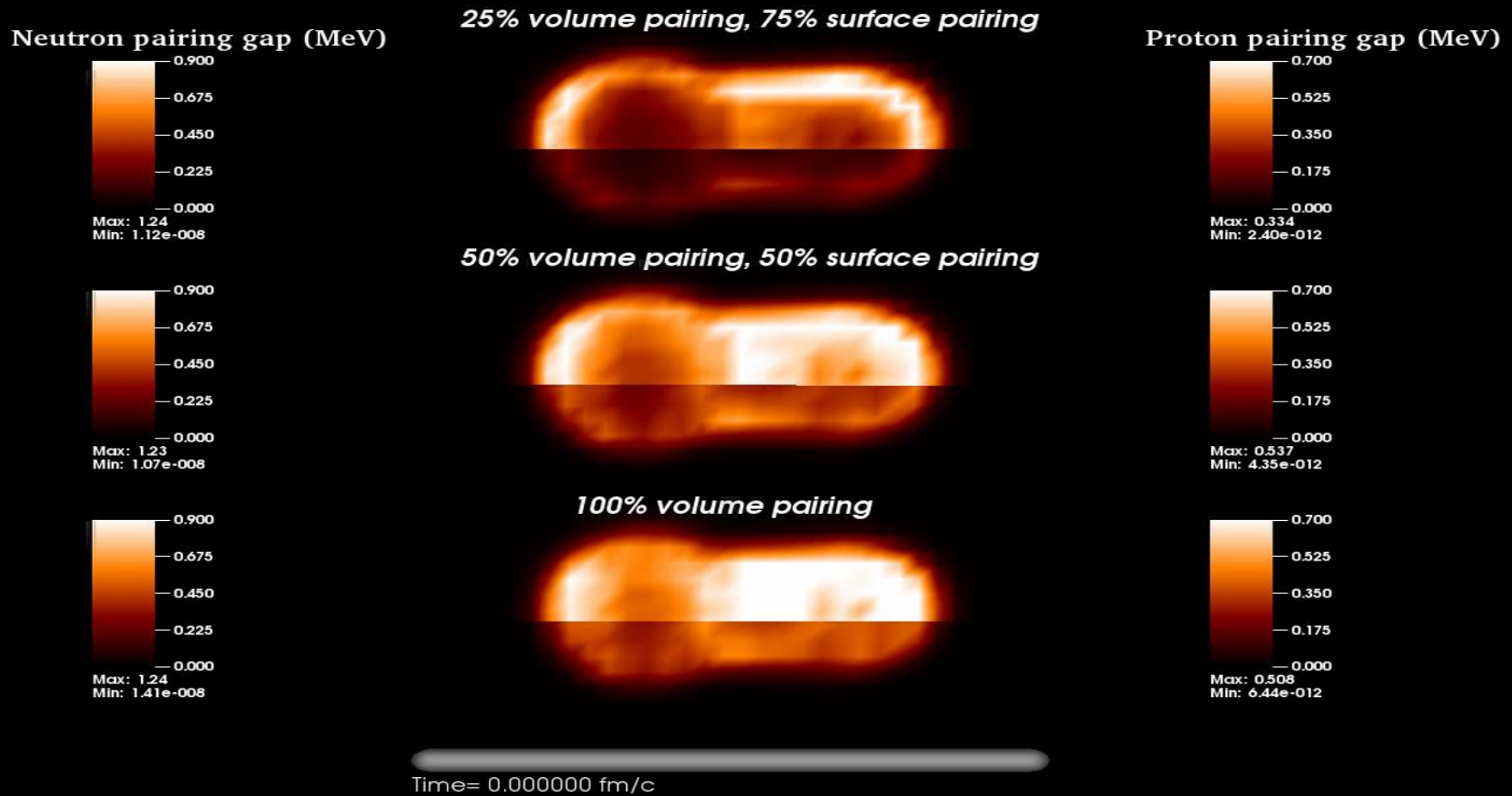


Evolution of the average magnitude of the pairing fields.



Hexadecapole (dashed), octupole (dotted), and quadrupole (solid) mass moments.

Fission of ^{240}Pu at excitation energy $E_x = 8.05; 7.91; 8.08$ MeV



$$1 \text{ zs} = 10^{-21} \text{ sec.} = 300 \text{ fm/c}$$

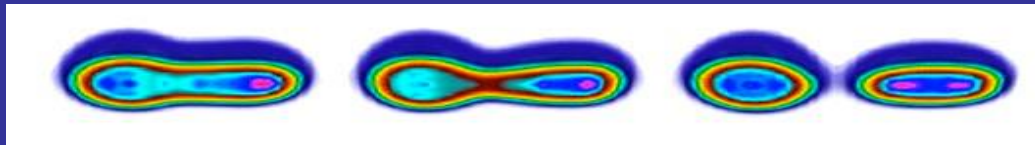
The most surprising finding was that the saddle-to-scission time was significantly longer than expected from any previous treatments.

Why?

The likeliest cause is the presence in TDSLDA of all possible collective degrees of freedom and that alone, even in the absence of dissipative effects can result in longer saddle-to-scission times.

The fluctuating pairing field might also cause this behavior.

- TDSLDA will offer insights into nuclear processes and quantities which are either not easy or impossible to obtain in the laboratory: fission fragments excitation energies and angular momenta distributions, element formation in astrophysical environments, other nuclear reactions ...
- TDSLDA offers an unprecedented opportunity to test the nuclear energy density functional for large amplitude collective motion, non-equilibrium phenomena, and in new regions of the collective degrees of freedom.
- The quality of the agreement with experimental observations is surprisingly good, especially taking into account the fact that we made no effort to reproduce any measured data.
- TDSLDA predicts long saddle-to-scission time scales and the systems behaves superficially as a very viscous one, while at the same time the collective motion is not overdamped. There is no thermalization and the "temperatures" of the fission fragments are not equal.
- It is straightforward to implement the Balian and Vénéroni recipe to compute two-body observables: fission fragments mass, charge, angular momenta, excitation energy widths, ...



Collisions of two superfluid nuclei

Physics of two nuclear, coupled superconductors

Little bit of history:

Volume 1, number 7

PHYSICS LETTERS

1 July 1962

POSSIBLE NEW EFFECTS IN SUPERCONDUCTIVE TUNNELLING *

B. D. JOSEPHSON

Cavendish Laboratory, Cambridge, England

Received 8 June 1962

We here present an approach to the calculation of tunnelling currents between two metals that is sufficiently general to deal with the case when both metals are superconducting. In that case new effects are predicted, due to the possibility that electron pairs may tunnel through the barrier leaving the quasi-particle distribution unchanged.

$$J(t) = J_c \sin(\Delta\varphi(t))$$

$$\frac{d(\Delta\varphi)}{dt} = \frac{2eU}{\hbar}$$

Dynamics of the Josephson effect:

AN ANALOG OF THE JOSEPHSON EFFECT IN NUCLEAR TRANSFORMATIONS

V. I. GOL'DANSKIĬ and A. I. LARKIN

Institute of Chemical Physics, Academy of Science, U.S.S.R.

Submitted March 30, 1967

Zh. Eksp. Teor. Fiz. 53, 1032-1037 (September, 1967)

When nuclei are bombarded by heavy ions, various processes of nucleon tunneling through the potential barrier that separates the interacting nuclei at the smallest possible classical distance are observed. It is shown that nucleon pairing may give rise to a significant increase of the cross section for the transition of neutron or proton pairs, a phenomenon which in some respects is analogous to the Josephson effect in superconductors. Pairing is taken into account in the calculation of the probability for the excitation of various levels by one-nucleon exchange, which has been calculated earlier by Breit and Ebel^[1] without such corrections. The probability for two-nucleon exchange is determined. An expression is obtained for the two-proton radioactivity with account of any number of arbitrary levels, which goes over into the Galitskii-Chel'tsov formula^[2] in the limiting case of a single S level.

Volume 32B, number 6

PHYSICS LETTERS

17 August 1970

ON A NUCLEAR JOSEPHSON EFFECT IN HEAVY ION SCATTERING

K. DIETRICH

Niels Bohr Institute, Copenhagen, Denmark*

Received 3 June 1970

The transfer of a pair of nucleons in sub-Coulomb scattering of two heavy ions is treated in a semi-classical theory. If both reaction partners are superconducting, a large enhancement factor is found.

Brief Reports

Brief Reports are short papers which report on completed research or are addenda to papers previously published in the Physical Review. A Brief Report may be no longer than $3\frac{1}{2}$ printed pages and must be accompanied by an abstract.

Weak evidence for a nuclear Josephson effect in the $^{34}\text{S}(^{32}\text{S}, ^{32}\text{S})$ elastic scattering reaction

Michel C. Mermaz

*Service de Physique Nucléaire—Métrologie Fondamentale, Centre d'Etudes Nucléaires de Saclay,
91191 Gif-sur-Yvette Cedex, France*

(Received 30 March 1987)

Optical model and exact finite range distorted-wave Born approximation analyses were performed on neutron pair exchange and alpha particle exchange reactions between two identical colliding cores. The possibility of a nuclear Josephson effect is discussed.

Neutron pair and proton pair transfer reactions between identical cores in the sulfur region

Michel C. Mermaz

Commissariat à l'Energie Atomique, Service de Physique Nucléaire, Centre d'études de Saclay, 91191 Gif sur Yvette, Cedex, France

Michel Girod

Commissariat à l'Energie Atomique, Service de Physique et Techniques Nucléaires, Boîte Postale 12, 91680 Bruyères-le-Châtel, France

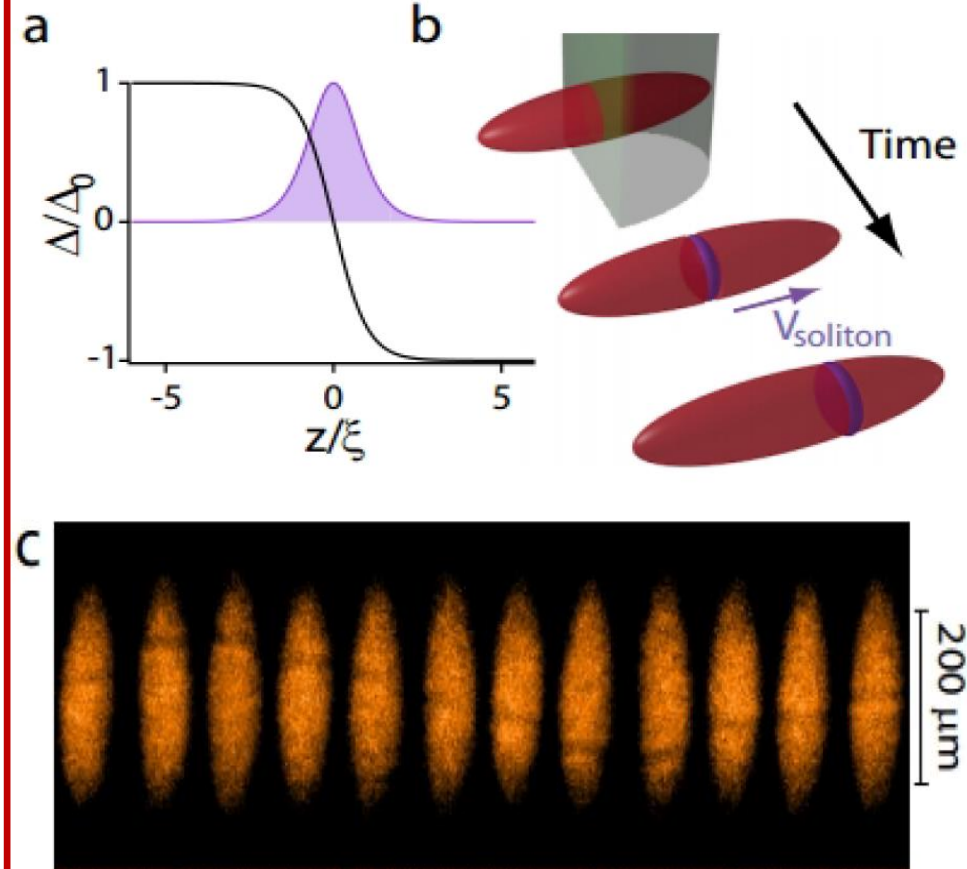
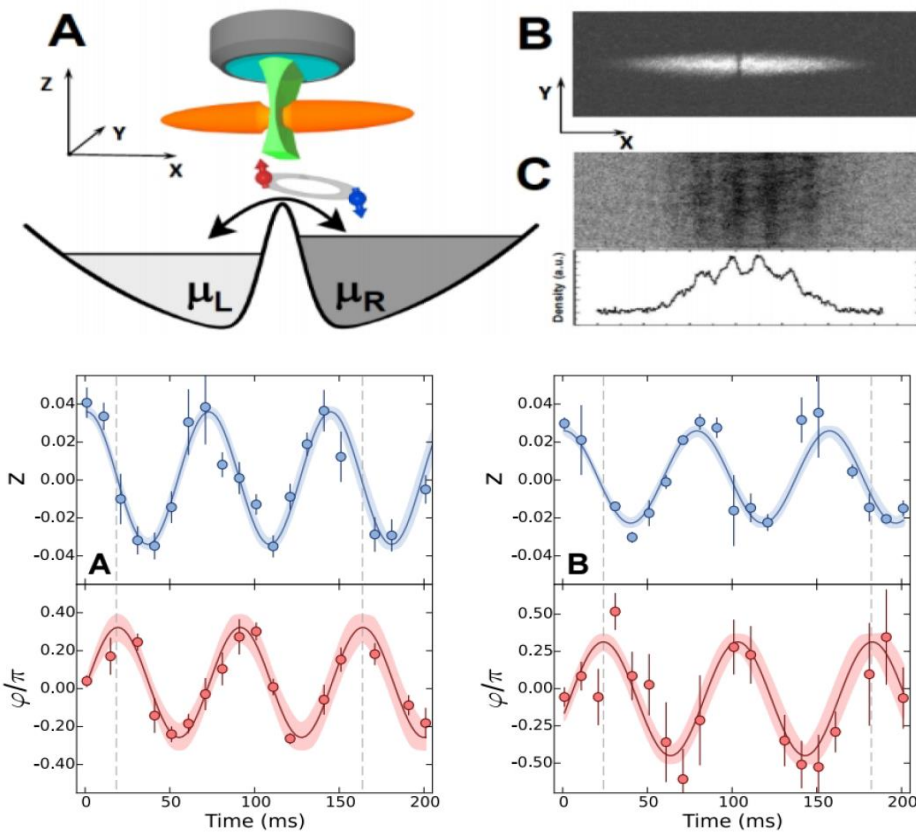
(Received 1 December 1995)

Optical model and exact finite range distorted-wave Born approximation analyses were performed on neutron pair exchange between identical cores for ^{32}S and ^{34}S nuclei and on proton pair exchange between identical cores for ^{30}Si and ^{32}S . The extracted spectroscopic factors were compared with theoretical ones deduced from Hartree-Fock calculations on these pairs of nuclei. The enhancement of the experimental cross sections with respect to the theoretical ones strongly suggests evidence for a nuclear Josephson effect.

Ultracold atomic gases: two regimes for realization of the Josephson junction

Weak coupling (weak link)

Strong coupling



Observation of **AC Josephson effect** between two 6Li atomic clouds.

It need not to be accompanied by creation of a topological excitation.

G. Valtolina et al., Science 350, 1505 (2015).

Creation of a „heavy soliton“ after merging two superfluid atomic clouds.

T. Yefsah et al., Nature 499, 426 (2013).

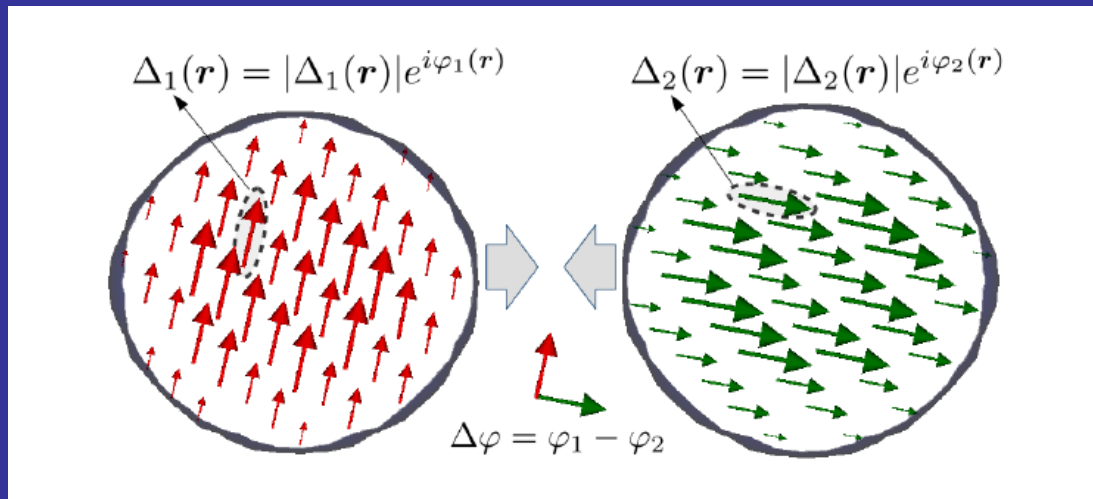
Usually, nuclear applications are limited to the first regime (weak link) and focused on the detection of the Josephson current in the form of enhanced cross section for pair transfer.

We are, however, interested in the **second regime** and nuclear collisions **ABOVE** the barrier.

Consequently the main questions are:

- how a possible solitonic structure can be manifested in nuclear system?
- what observable effect it may have on heavy ion reaction:
kinetic energy distribution of fragments, capture cross section, etc.?

Clearly, we cannot control phases of the pairing field in nuclear experiments and the possible signal need to be extracted after averaging over the phase difference.



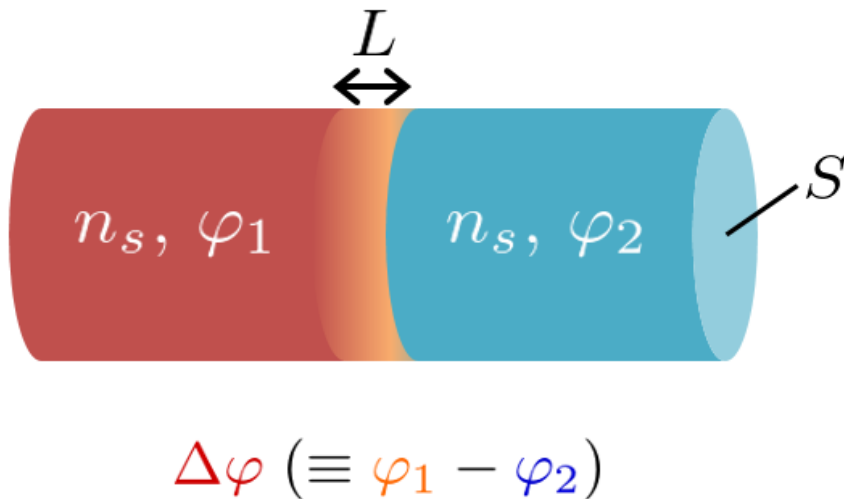
Y. Hashimoto, G. Scamps, Phys. Rev. C94, 014610(2016) - TDHFB studies of 20O+20O reaction produced negligible effect.

Estimates for the magnitude of the effect

At first one may think that the magnitude of the effect is determined by the nuclear pairing energy which is of the order of MeV's in atomic nuclei (according to the expression):

$$\frac{1}{2} g(\varepsilon_F) |\Delta|^2; \quad g(\varepsilon_F) - \text{density of states}$$

On the other hand the energy stored in the junction can be estimated from Ginzburg-Landau (G-L) approach:

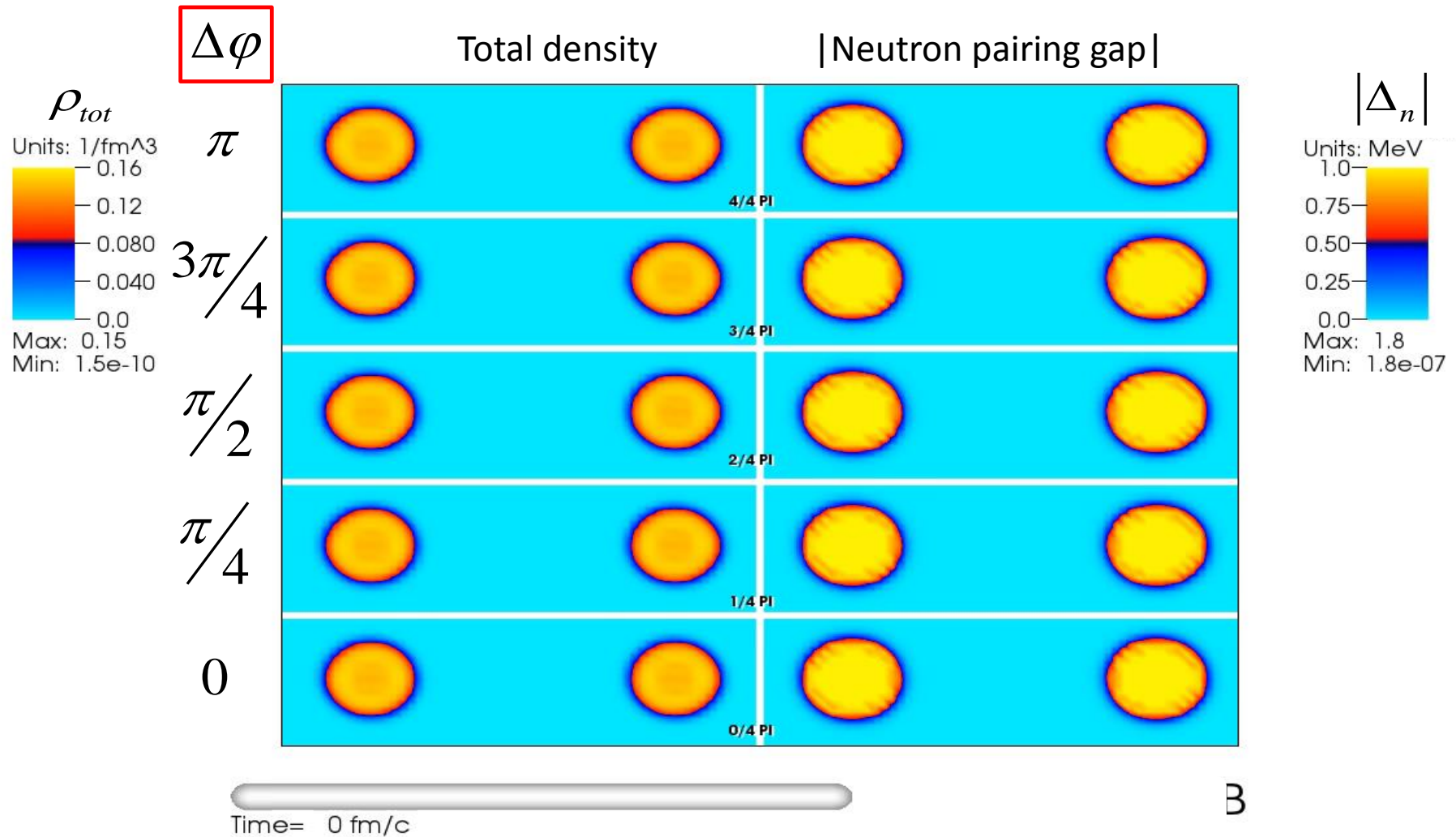


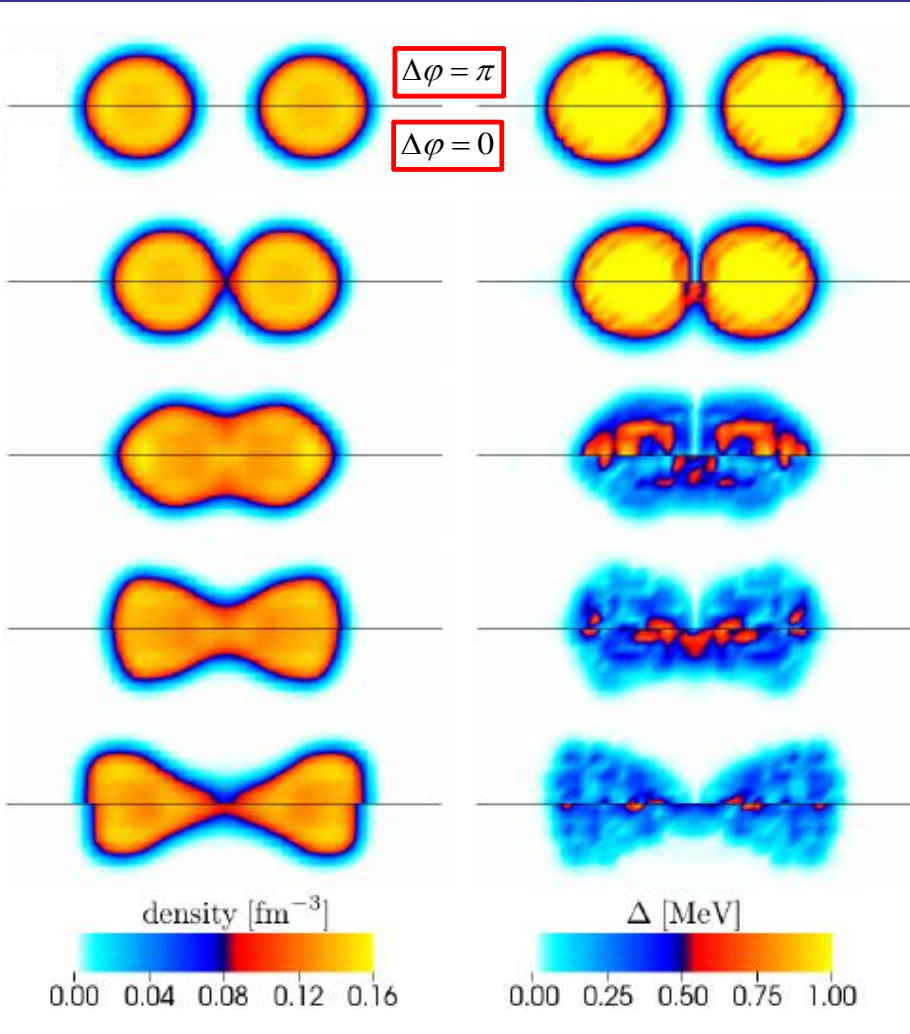
$$E_j = \frac{S \hbar^2}{L 2m} n_s \sin^2 \frac{\Delta\varphi}{2}$$

For typical values characteristic for two heavy nuclei:

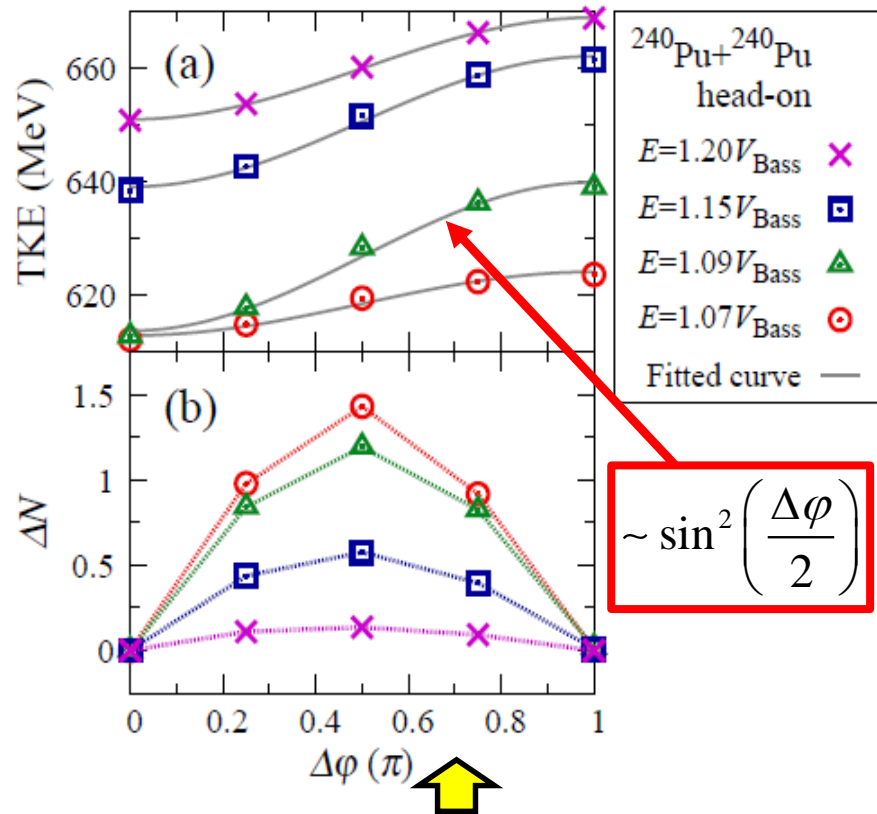
$$E_j \approx 30 \text{ MeV}$$

$^{240}\text{Pu} + ^{240}\text{Pu}$ at energy $E \approx 1.1V_{\text{Bass}}$





Total kinetic energy of the fragments (TKE)



Creation of the solitonic structure between colliding nuclei prevents energy transfer to internal degrees of freedom and consequently enhances the kinetic energy of outgoing fragments.

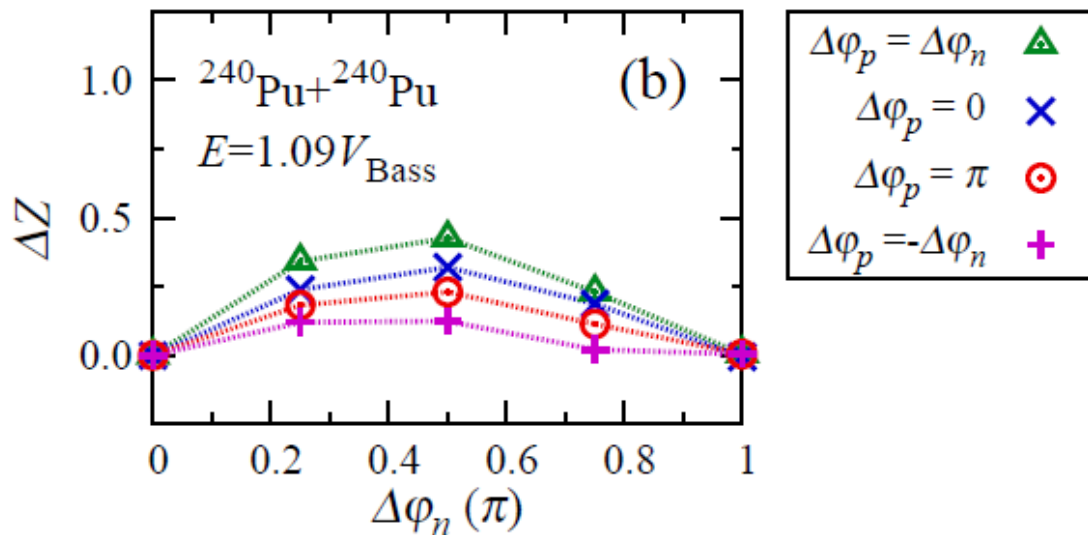
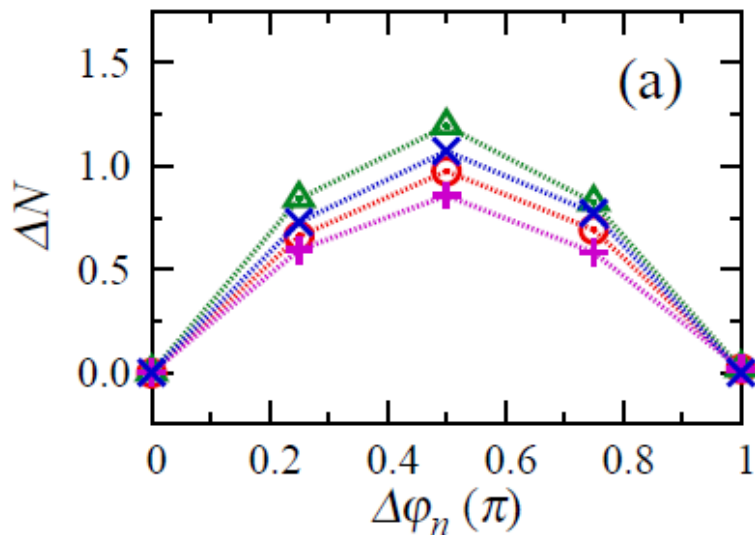
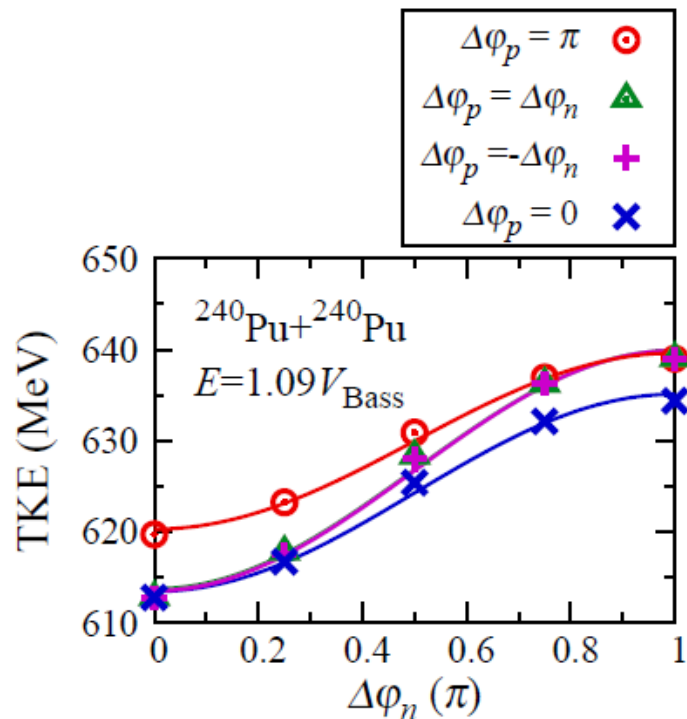
Surprisingly, the gauge angle dependence from the G-L approach is perfectly well reproduced in the kinetic energies of outgoing fragments!

Proton pairing gap contribution to TKE

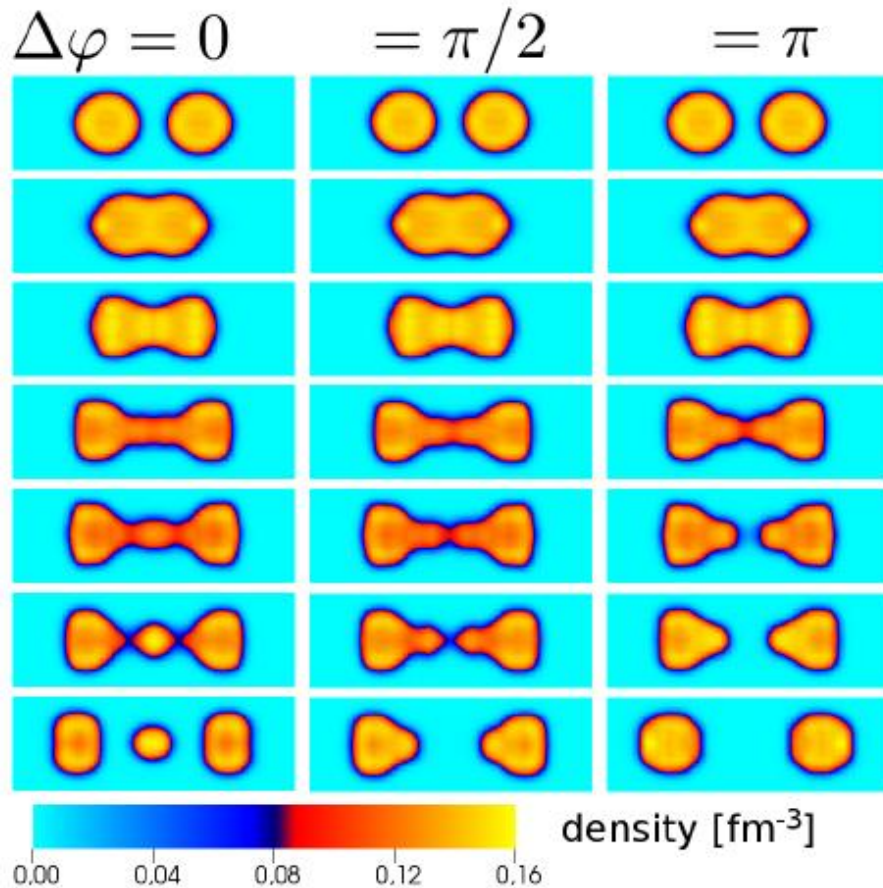
The effect is predominantly due to neutron pairing.

Neutron transfer

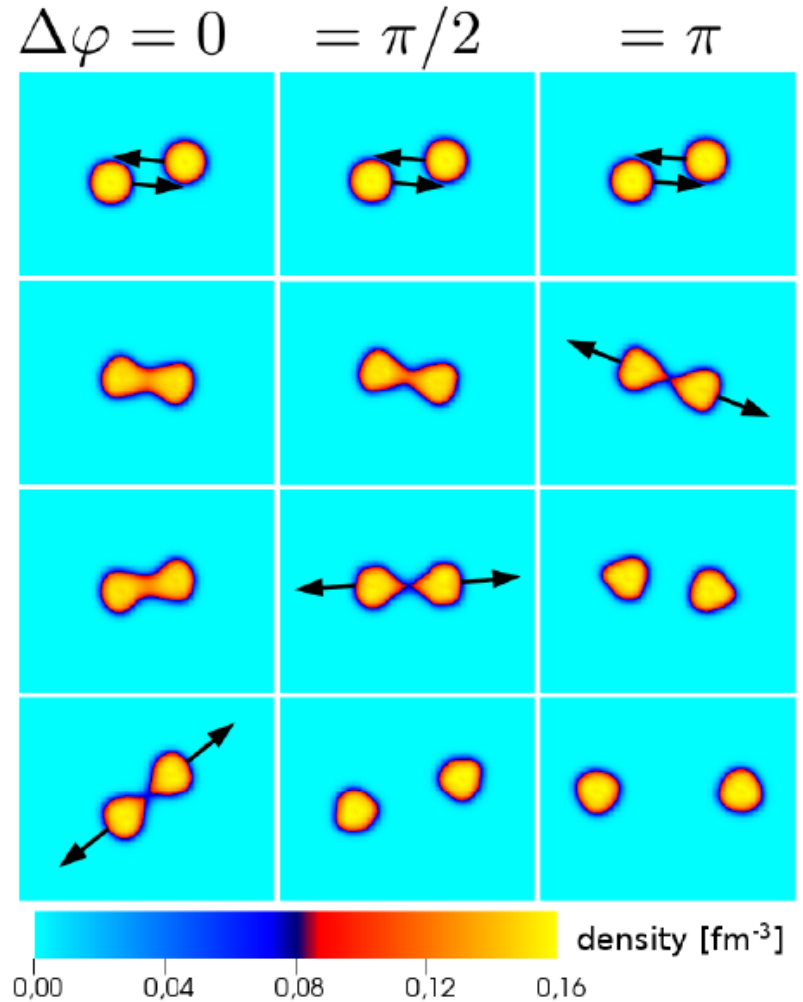
Proton transfer



Noncentral collisions



At higher energies (1.3-1.5 of the barrier height) the phase difference modifies the reaction outcomes suppressing the reaction channel leading to 3 fragments.



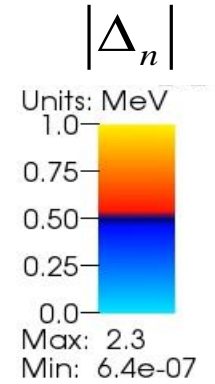
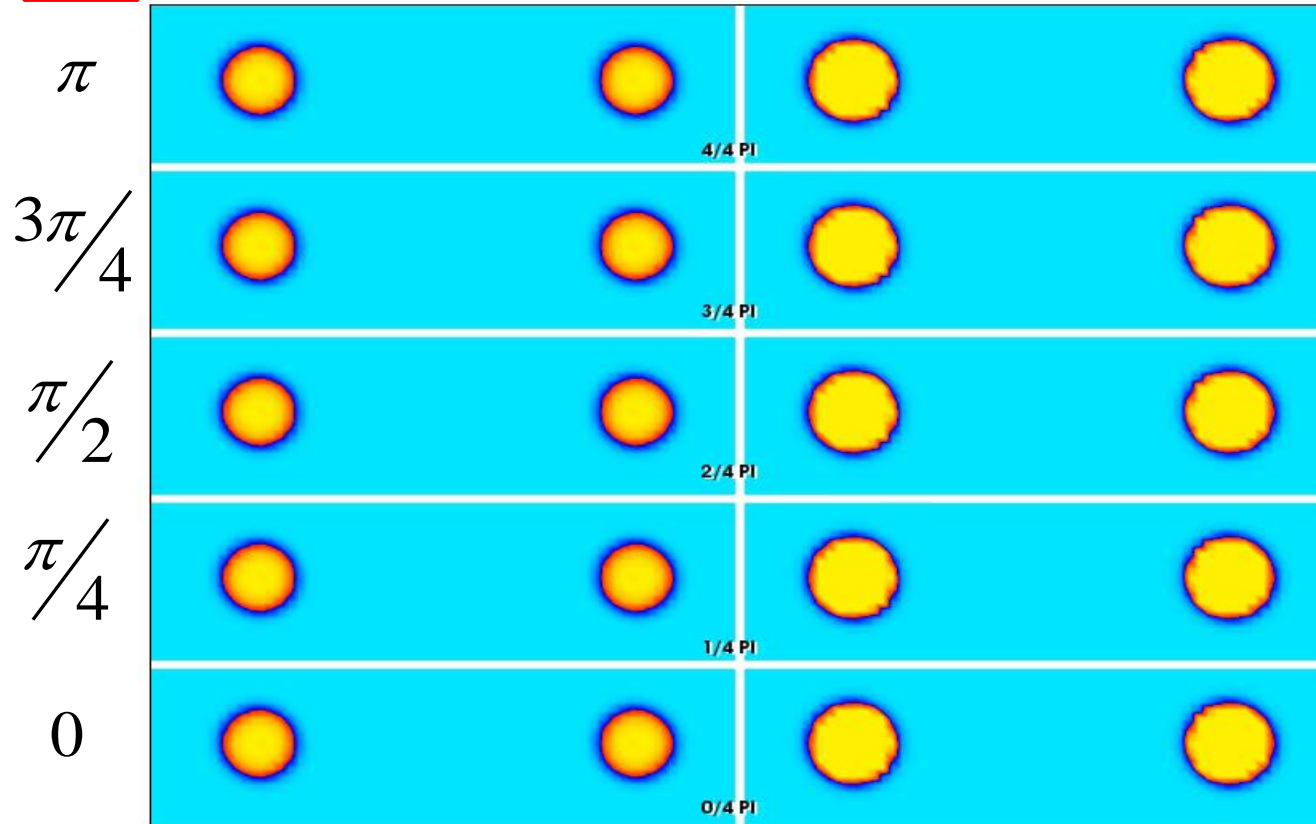
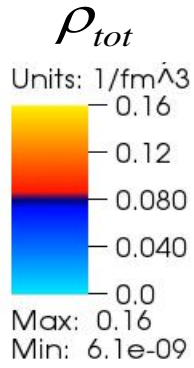
For noncentral collisions the trajectories of outgoing nuclei are affected due to the shorter contact time for larger phase differences.

$^{90}\text{Zr} + ^{90}\text{Zr}$ at energy $E \approx V_{\text{Bass}}$

$\Delta\varphi$

Total density

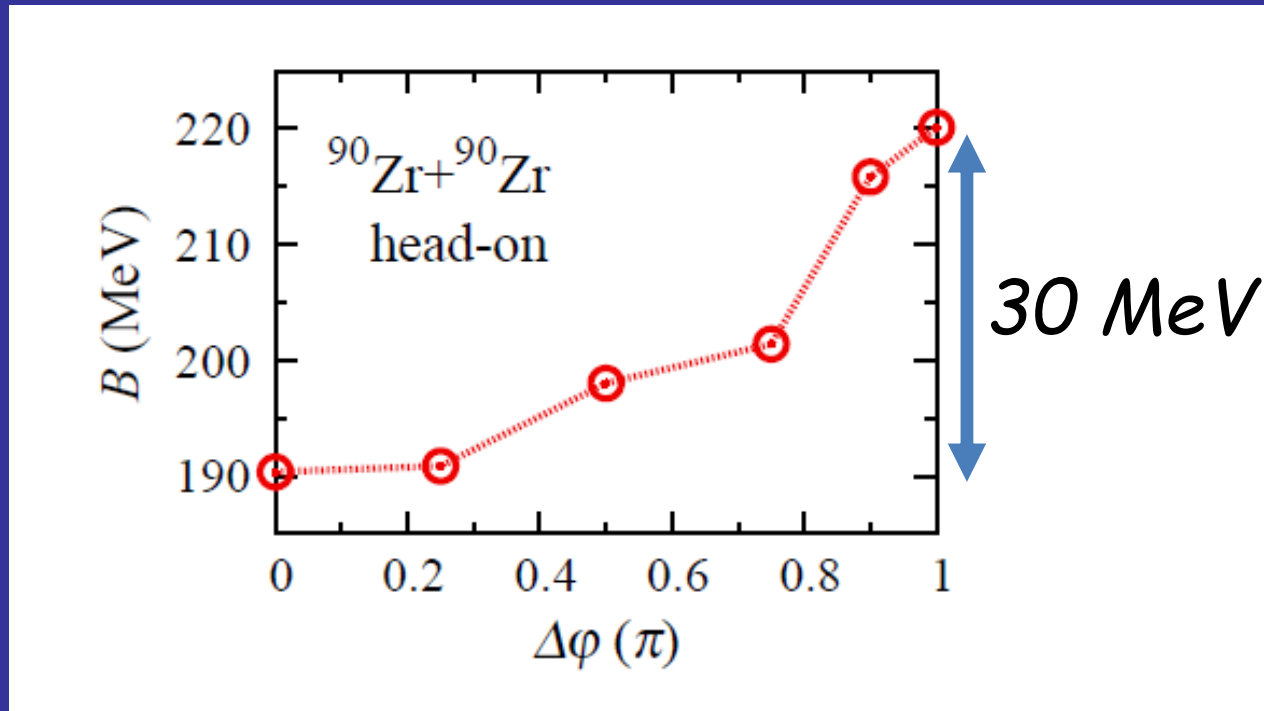
|Neutron pairing gap|



Time= 0 fm/c

Modification of the capture cross section!

Effective barrier height for fusion as a function of the phase difference



What is an average extra energy needed for the capture?

$$E_{extra} = \frac{1}{\pi} \int_0^{\pi} (B(\Delta\phi) - V_{Bass}) d(\Delta\phi) \approx 10 \text{ MeV}$$

How the angle dependence affects the shape of the excitation function?

$$\frac{d}{dE} (E\sigma(E)) \propto \Delta\phi_{tr} + \dots$$

Summarizing

Pairing field dynamics play an important role in nuclear dynamics including both induced fission and collisions.

Clearly the aforementioned effects **CANNOT** be grasped by any version of simplified (and commonly used) TDHF+BCS approach.

The phase difference of the pairing fields of colliding medium or heavy nuclei produces a similar solitonic structure as the system of two merging atomic clouds.

The energy stored in the created junction is subsequently released giving rise to an increased kinetic energy of the fragments and modifying their trajectories. The effect is found to be of the order of 30MeV for heavy nuclei and occur for energies up to 20-30% of the barrier height.

Consequently the effective barrier for the capture of medium nuclei is enhanced by about 10MeV.

Josephson current is weak and DOES NOT contribute noticeably to collision dynamics (consistent with other studies).

Open questions

Time dependent DFT describes nuclear collision in the broken symmetry framework.

What is the effect of the particle nonconservation ?

Summarizing

- TDDFT extended to superfluid systems and based on the local densities offers a flexible tool to study quantum superfluids far from equilibrium.
- Future plans:
- Ultracold atoms: investigation of quantum turbulence in Fermi systems; topological excitations in spin-polarized atomic gases in the presence of LOFF phase.
- Neutron star: Provide a link between large scale models of neutron stars and microscopic studies; towards the first simulation of the glitch phenomenon based on microscopic input.
- Nuclear physics: induced fission and fusion processes - pin down the role pairing dynamics; search for new effects related to pairing dynamics in nuclear collisions and creation of superheavies.

Selected supercomputers (CPU+GPU) currently in use:

INTRODUCING TITAN

Advancing the Era of Accelerated Computing



Titan: 27 PFlops

Tsubame: 5.7 PFlops



TSUBAME

Piz Daint: 7.787 PFlops

